Deep Inelastic Scattering:

Measuring the Parton Structure of the Proton using Inclusive Lepton-Hadron collisions

Jon Pumplin

Michigan State University

CTEQ Summer School -- Beijing 2014

High Energy collisions can be calculated in the standard model, PROVIDED that they involve a large momentum transfer, which corresponds to a short distance scale according to quantum mechancs.

The Asymptotic Freedom property of QCD makes the strong coupling small for short distance processes, so perturbation theory (LO, NLO, NNLO, + resummation) can be used.

Examples: at LHC, Higgs production is computed at NNLO; Inclusive Jet production is computed at NLO, with NNLO coming soon; Total cross section can't be computed at all.

Typical processes of interest at Hadron Colliders such as LHC result from a hard interaction between just two partons (quarks or gluons): one from each of the two colliding hadrons.

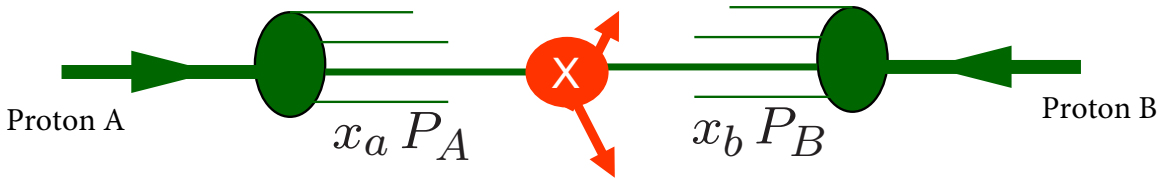

$$\sigma_X = \sum_{a\,b} \int_0^1 dx_a\, f_{a\in A}(x_a,\mu) \int_0^1 dx_b\, f_{b\in B}(x_b,\mu)\, \hat{\sigma}_{a\,b\to X}(\mu)$$

The Parton Distribution Function $f_{a\in A}(x_a,\mu)$ is the probability density to find a parton with flavor a in proton A, with momentum fraction xa at scale mu.

Relatively little attention has been paid to "multi-parton" interactions, in which more than one of the partons in a single hadron are involved in a hard scattering. Such processes are important in estimating Underlying Event backgrounds, as well as being a rich potential source of information on nonperturbative proton structure.

Considerable work has been done on generalizations of the traditional parton distributions in which the distribution in transverse momentum of the parton is included along with the distribution in momentum fraction. The correlation between transverse momentum and longitudinal momentum fraction is important for understanding and fitting the full range of the transverse momentum distributions, e.g., of W and Z.

Considerable work has also been done on generalizing parton distributions to the partons in a polarized proton. This will be of interest when the 12GeV upgrade at JLAB is running.

Complications

1. The PDfs and the hard cross section contain infinities from colinear and soft singularities. These are tamed by dimensional regularization, and cancelled throught the magic of renormalization, with the introduction of a Renormalization scale and a Factorization scale --- see other lectures at the School.

2. If we could calculate to all orders in perturbation theory, the results would be independent of scale choice mu. In practice, we take mu to be approximately the hardness scale of the interaction under study, which reduces the sensitivity to it; and we use the sensitivity to changes in mu as a measure of the theoretical uncertainty.

$$\sigma_X = \sum_{a\,b} \int_0^1 dx_a\, f_{a\in A}(x_a,\mu) \int_0^1 dx_b\, f_{b\in B}(x_b,\mu)\, \widehat{\sigma}_{a\,b\to X}(\mu)$$

Deep Inelastic Scattering refers to large momentum transfer (short distance) collisions between a LEPTON and a hadron:

$$\sigma_{A\,B\to C\,X} = \int_0^1 dx_b\, f_{b\in B}(x_b,\mu)\ \hat{\sigma}_{A\,b\to C\,X}(\mu)$$

The whole lepton participates in the hard scattering, in a way that can be calculated reliably by perturbation theory; and the smallness of electroweak couplings guarantees that only one parton from the hadron is involved in the hard scattering. DIS is therefore an excellent source of information on $f_{b\in B}(x_b,\mu)$.

Kinematics of DIS

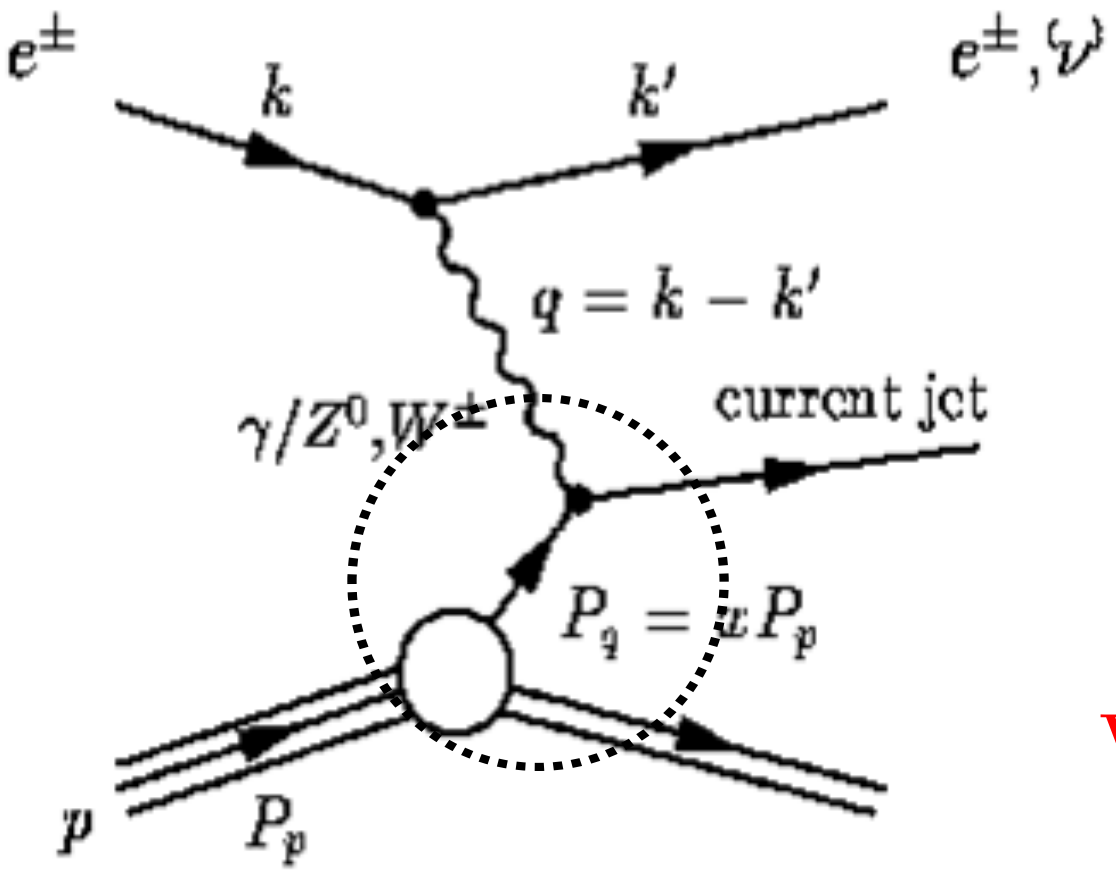

$$s = (k + p)^2$$

$$Q^2 = -q^2 = -(k - k')^2$$

$$x = \frac{Q^2}{2\,q\cdot p}$$

$$y = \frac{q\cdot p}{k\cdot p} = \frac{Q^2}{x\,s}$$

$$W^2 = (q + p)^2 = m_p^2 + \left(\frac{1-x}{x}\right) Q^2$$

$e^- p \to e^- X$ has three independent kinematic variables, **e.g.**

E, E', θ of electron in proton rest frame. **Preferred choice:**

s = CM energy squared: set by accelerator design

Q^2 = momentum transfer squared: distance probed $\sim \hbar/Q$

$x = x_{\rm Bj}$ = parton mom**entum** fraction in ∞-mom**entum** frame

Q. Why is x the momentum fraction of the parton?

A. Actually x is more precisely the fraction of the large "+" or "-" momentum $E \pm P_z$ in the ∞-momentum frame.

Let $p_{\rm i}$ and $p_{\rm f}$ be the initial and final momenta of the struck parton. Momentum conservation gives $q + p_{\rm i} = p_{\rm f}$.

Squaring both sides gives $q^2 + 2q \cdot p_{\rm i} + {p_{\rm i}}^2 = {p_{\rm f}}^2$.

At large $Q^2 = -q^2$ we can ignore ${p_{\rm i}}^2$ and ${p_{\rm f}}^2$, so $Q^2 = 2q \cdot p_{\rm i}$.

Also, $p_{\rm i} = x p_{\rm target}$ for the large "+" (or "-") component by the definition of x.

From this argument, you can see that if Q^2 is not very large, there can be important mass corrections, e.g., in neutrino DIS for hard scattering processes like $W^+ s \to c$.

Asymptotic freedom and infrared slavery

In the infinite momentum frame, or any frame where the proton has a very large momentum, the interactions between the partons that creates the proton bound state are slowed down by the time dilation effect of relativity. Hence it is plausible that the partons interact like free particles with the short distance (large Q) probe in DIS.

The asymptotic freedom property of QCD is crucial to this: the binding interactions are weak at short distance because alpha_s goes to zero in that limit.

Meanwhile, the partons must hadronize after the hard interaction, because alpha_s becomes large at large distances.

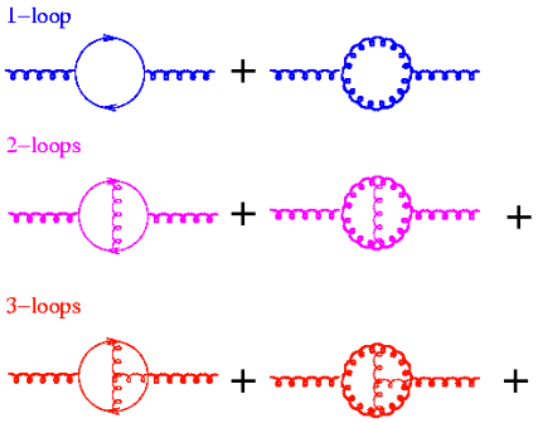

$$\alpha_s = \frac{12\pi}{(33 - 2n_f)\log\frac{Q^2}{\Lambda^2_{qcd}}} \quad \text{(1-loop)}$$

Kinematic Region for DIS

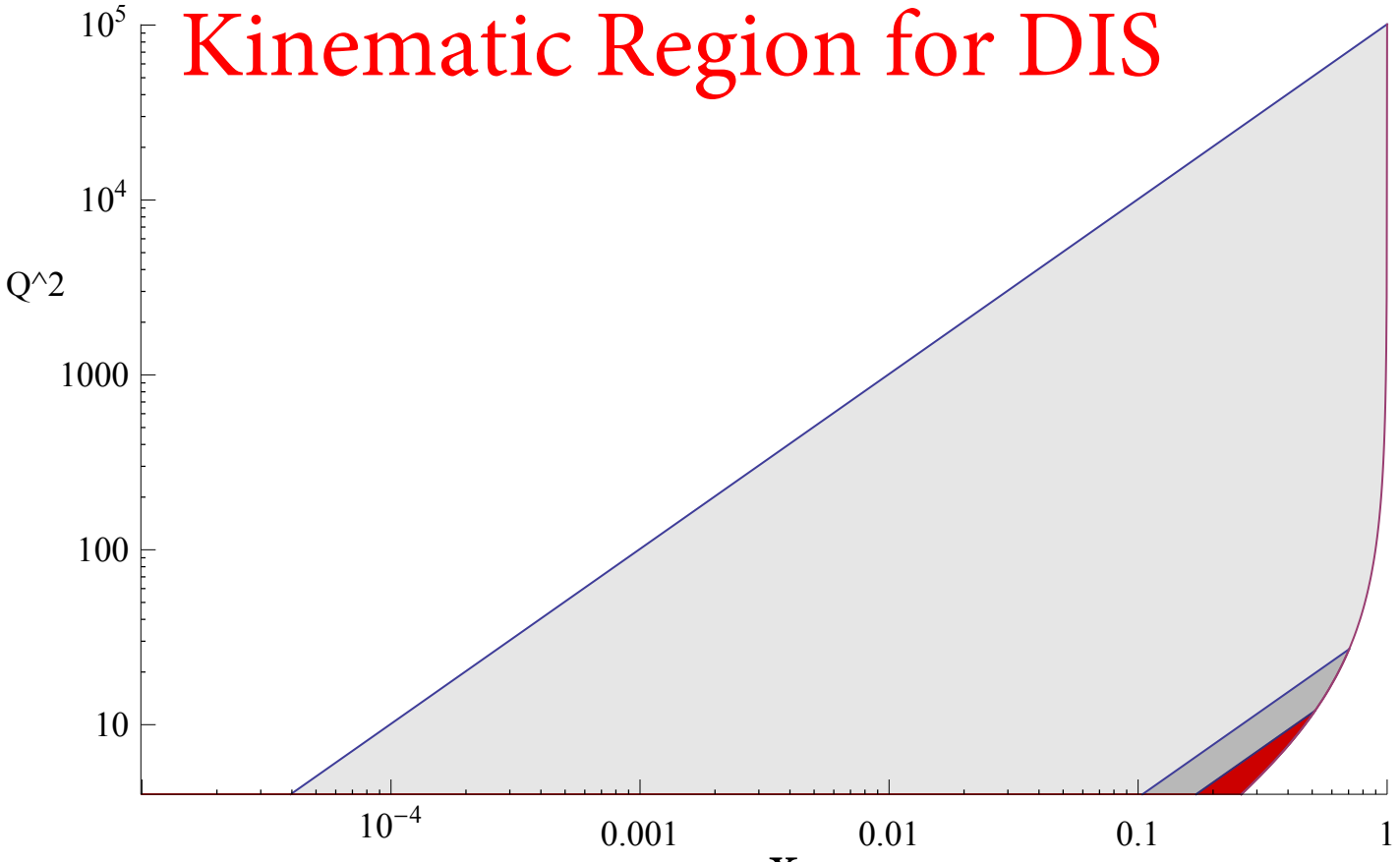

Kinematic limit: $x < 1,\ y < 1 \implies Q_2 < s$

Perturbative requirement: $Q > 2\,\text{GeV}$ (standard CTEQ cut)

Avoid "resonance region": $W > 3.5\,\text{GeV}$ (standard CTEQ cut)

Light shaded: HERA 27.5 GeV $e^{\pm}$ on 920 GeV p, $\sqrt{s} = 318$ GeV.

Dark shaded : SLAC (1967–72) 20 GeV e^- fixed target, $\sqrt{s} = 6.2$ GeV

Red shaded: JLAB/CEBAF **12GeV** upgrade (2015?) $\sqrt{s} = 4.8$ GeV

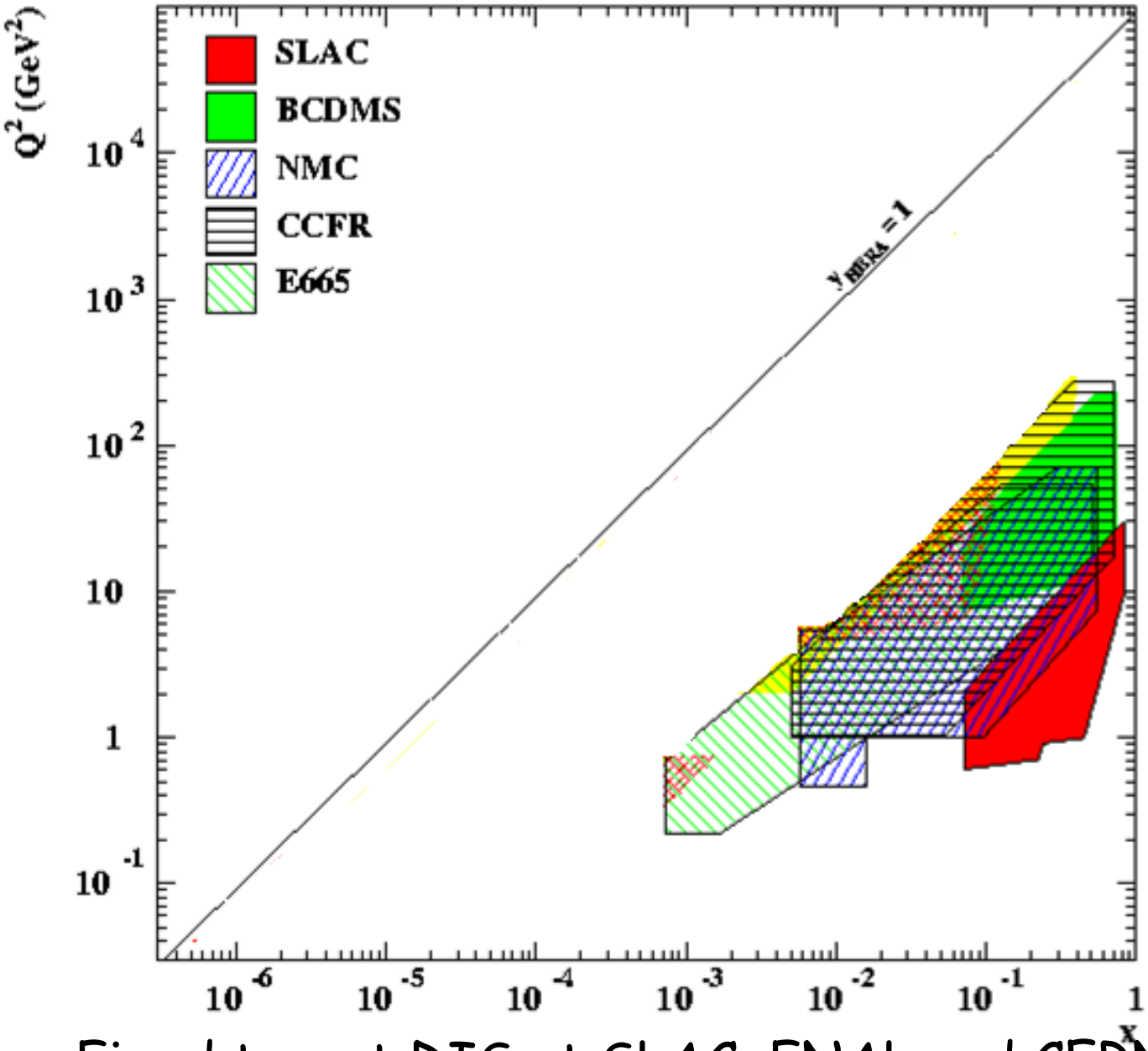

Fixed target DIS at SLAC, FNAL and CERN completed ~ 10-25 years ago.

(Plot includes low Q^2 non-perturbative region.)

Electron and muon DIS experiments

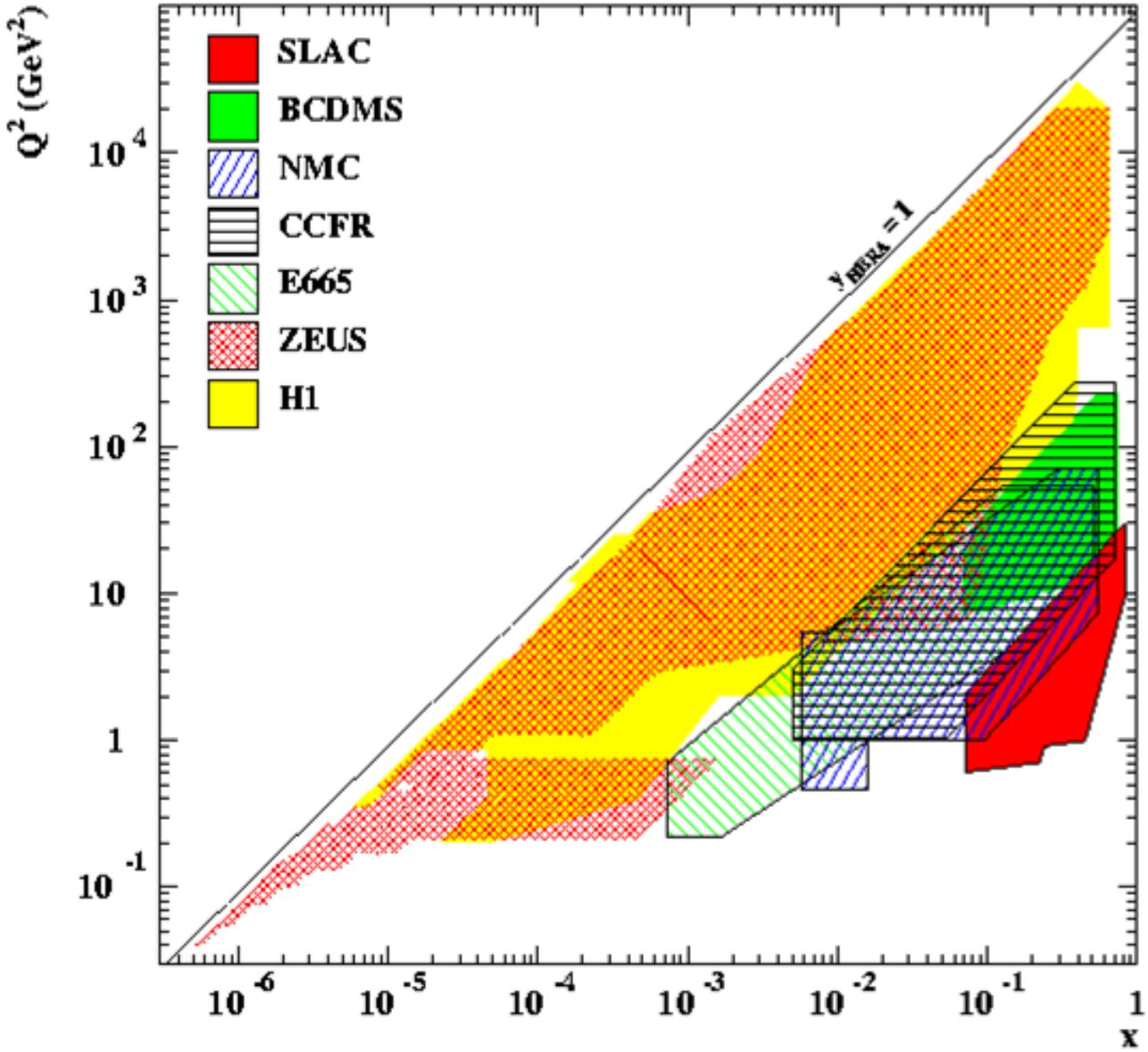

HERA: H1 and ZEUS experiments 1992 – 2007

Combined data analysis nearly finished?

Kinematic Map for LHC

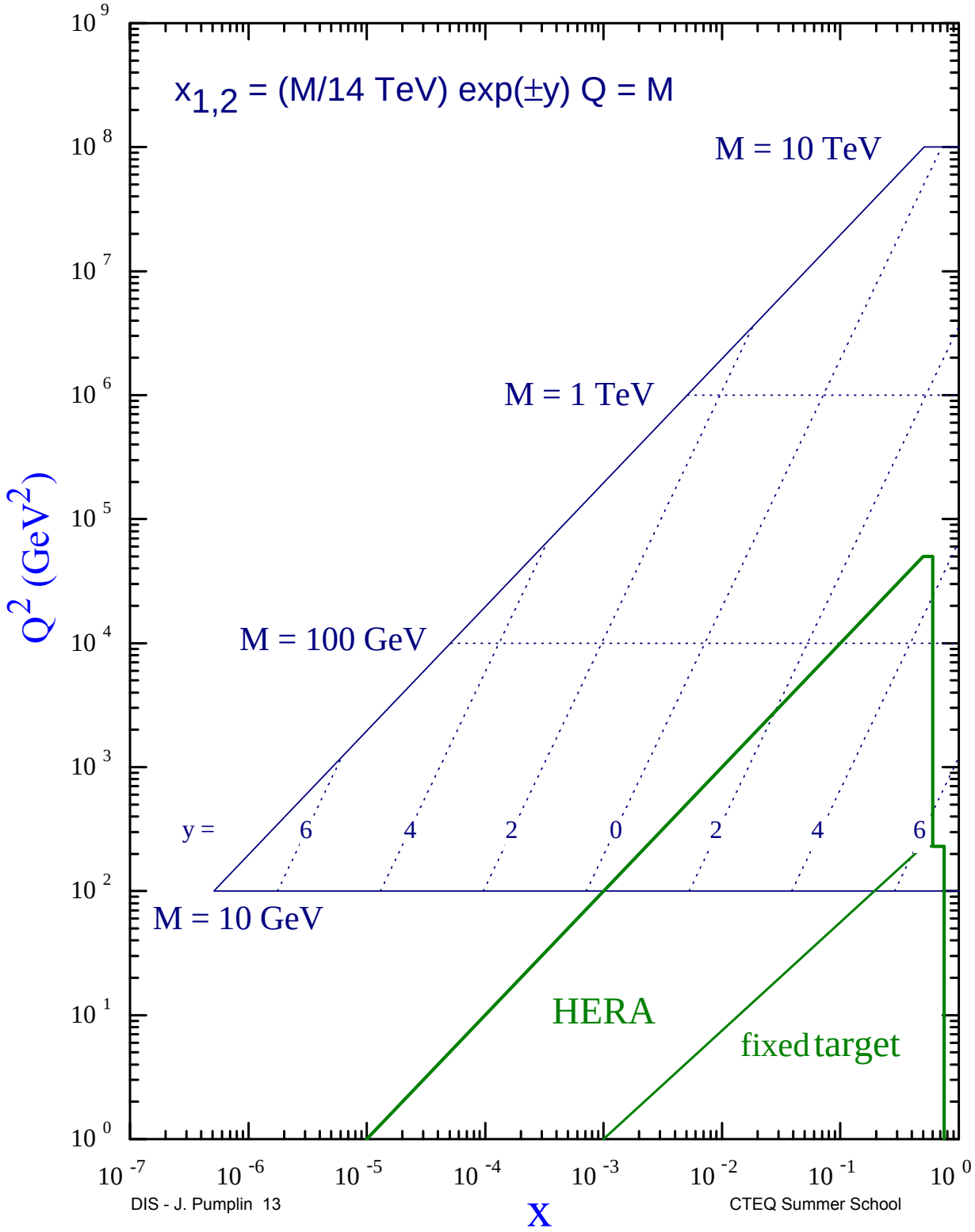

LHC probes parton distributions far outside the region where they are measured in DIS.

DGLAP evolution allows perturbative calculation of PDFs at large Q from measurements at small Q . The evolution involves branching, so small-x behavior is partly predictable from larger x at smaller Q .

Nevertheless, the large uncertainty of PDFs at small x in the HERA region, and the possible breakdown of DGLAP at small x leads to an exciting region of small-x physics to explore at LHC.

Basic DIS Formalism

(leading order in EW coupling; no QCD assumption)

Lepton-hadron scattering process

$$\ell_1(\ell_1) + N(P) \longrightarrow \ell_2(\ell_2) + X(P_X)$$

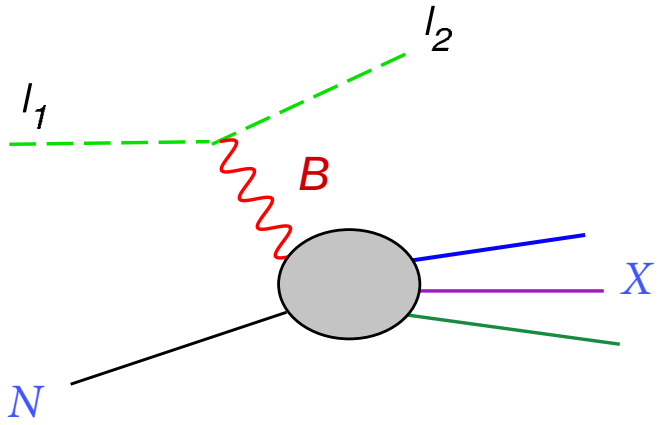

(B = g, W, Z)

Effective fermion-boson electro-weak interaction Lagrangian:

$$\mathcal{L}_{\rm int}^{\rm EW} = -g_B \left[j_\mu^{(\ell)}(x) + J_\mu^{(h)}(x) \right] \; V_B^\mu(x)$$

EW SU(2)xU(1) gauge coupling constants

B	γ	$W^\pm$	Z
g_B	$-e$	$\frac{g}{2\sqrt{2}}$	$\frac{g}{2\cos\theta_W}$

Basic Formalism: current operators and couplings

Fermion current operator:

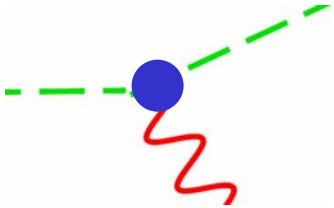

$$J_\mu^{(f)}(x) = \overline{\psi}_f(x)\gamma_\mu\,(g_V - g_A\gamma^5\,)\psi_f(x)$$
$$= \overline{\psi}_f(x)\gamma_\mu\,[g_R(1+\gamma^5\,) + g_L(1-\gamma^5\,)]\psi_f(x)$$

V-A couplings:

or,

Left-right (chiral) couplings:

Charge

Weak isospin

Weinberg angle

CKM mixing matrix

	γ	Z	$W^\pm$
g_V	Q_i	$T_{3L}^i - 2Q_i \sin^2\theta_W$	$1 \cdot V_{ij}$
g_A	0	T_{3L}^i	$1 \cdot V_{ij}$
g_R	$\frac{Q_i}{2}$	$-Q_i \sin^2\theta_W$	0
g_L	$\frac{Q_i}{2}$	$T_{3L}^i - Q_i \sin^2\theta_W$	$1 \cdot V_{ij}$

Basic Formalism: Scattering Amplitudes

Scattering Amplitudes

$$\mathcal{M} = J^*_\mu(P,q)\frac{g_B^2 G^\mu{}_\nu}{Q^2+M_B^2}j^\nu(q,\ell)$$

Spin 1 projection tensor $G^\mu{}_\nu = g^\mu{}_\nu - q^\mu q_\nu/M_B^2.$

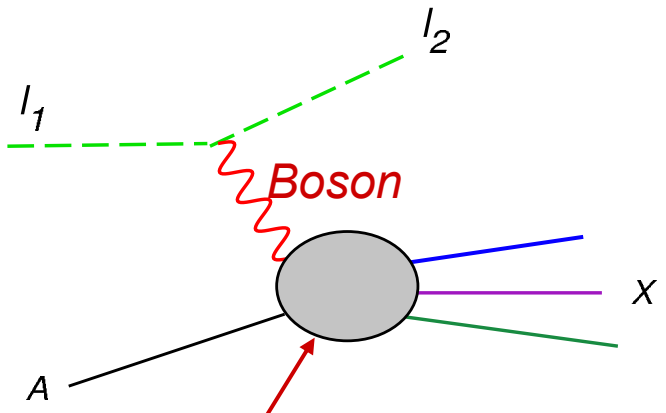

Lepton current amplitude (known):

$$j^\mu(q,\ell) = \langle \ell_2|j^\mu|\ell_1\rangle = \overline{u}(\ell_2)\gamma^\mu[g_R(1+\gamma^5)+g_L(1-\gamma^5)]u(\ell_1)$$

Hadron current amplitude (unknown):

$$J^*_\mu(P,q) = \langle P_X|J^\dagger_\mu|P\rangle$$

Objects of study:

* Parton structure of the nucleon: (short distance)
* QCD dynamics at the confinement scale: (long distance)

Basic Formalism: Cross section

Cross section = (amplitude)^2 phase space / flux

$$d\sigma = \frac{G_1\, G_2}{2\Delta(s, m_{\ell_1}^2, M^2)}\, 4\pi Q^2\, L^\mu_\nu\, W^\nu_\mu\, d\Gamma$$

$$G_i = g_{B_i}^2/(Q^2 + M_{B_i}^2)$$

Lepton tensor (known):

$$L^\mu{}_\nu = \frac{1}{Q^2} \overline{\sum_{\text{spin}}} \langle \ell_1 | j^\dagger_\nu | \ell_2 \rangle \langle \ell_2 | j^\mu | \ell_1 \rangle$$

Hadron tensor (unknown):

$$W^\mu{}_\nu = \frac{1}{4\pi} \overline{\sum_{\text{spin}}} (2\pi)^4 \delta^4(P + q - P_X) \langle P | J^\mu | P_X \rangle \langle P_X | J^\dagger_\nu | P \rangle$$

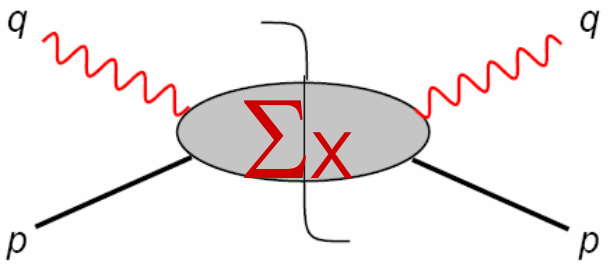

Object of study:

* Parton structure of the nucleon;
* QCD dynamics at the confinement scale

Basic Formalism: Structure Functions

Expansion of $W^{\mu}{}_{\nu}$ in terms of Lorentz structure

$$W^{\mu}{}_{\nu} = -g^{\mu}{}_{\nu}W_1 + \frac{P^{\mu}P_{\nu}}{M^2}W_2 - i\frac{\epsilon^{Pq\mu}{}_{\nu}}{2M^2}W_3 + \\ + \frac{q^{\mu}q_{\nu}}{M^2}W_4 + \frac{P^{\mu}q_{\nu} + q^{\mu}P_{\nu}}{2M^2}W_5 + \frac{P^{\mu}q_{\nu} - q^{\mu}P_{\nu}}{2M^2}W_6$$

Cross section in terms of the structure functions

$$\frac{d\sigma}{dE_2\, d\cos\theta} = \frac{2E_2^2}{\pi M}\frac{G_1\, G_2}{n_\ell}\left\{g^2_{+\,\ell}\left[2W_1\sin^2\frac{\theta}{2} + W_2\cos^2\frac{\theta}{2}\right] \pm g^2_{-\,\ell}\left[\frac{E_1+E_2}{M}W_3\sin^2\frac{\theta}{2}\right]\right\}$$

Charged Current (CC) processes (neutrino beams):

W-exchange (diagonal); left-handed coupling only; ….

Neutral Current (NC) processes (e,μ scat.)---low energy:
(fixed tgt): γ-exchange (diagonal); vector coupling only; …

Neutral Current (NC) processes (e,μ scat.)---high energy
(hera): γ & Z exchanges: G_1^2, G_1G_2, G_2^2 terms; ….

Basic Formalism: Scaling structure functions

Kinematic variables

$$\nu = \frac{P\cdot q}{\sqrt{P\cdot P}} = E_1 - E_2$$

$$x = \frac{-q^2}{2P\cdot q} = \frac{Q^2}{2M\nu}$$

$$y = \frac{P\cdot q}{P\cdot \ell_1} = \frac{\nu}{E_1}$$

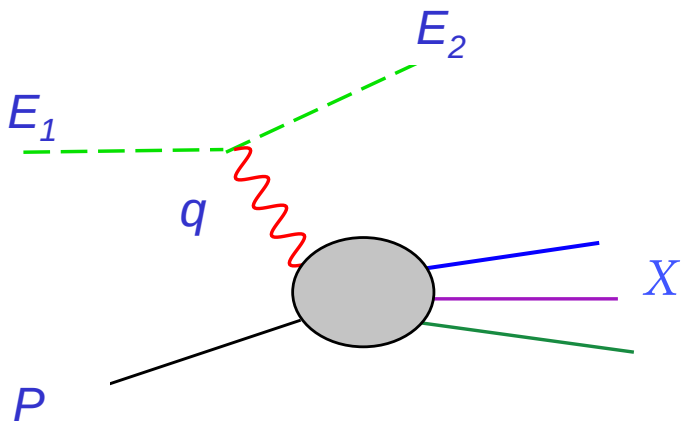

Scaling (dimensionless) structure functions:

$$F_1(x,Q) = W_1$$
$$F_2(x,Q) = \frac{\nu}{M}W_2$$
$$F_3(x,Q) = \frac{\nu}{M}W_3$$

Scaling form of cross section formula:

$$\left(g^2_{\pm\,\ell} = g^2_{L\,\ell} \pm g^2_{R\,\ell} \right)$$

$$\frac{d\sigma}{dxdy} = \frac{2ME_1}{\pi}\,\frac{G_1\,G_2}{n_\ell}\left\{ g^2_{+\,\ell}\left[xF_1\,y^2 + F_2\left[(1-y) - \left(\frac{Mxy}{2E_1}\right)\right]\right] \pm g^2_{-\,\ell}\left[xF_3\,y(1-\frac{y}{2})\right]\right\}$$

n_ℓ is the number of polarization states of the incoming lepton

Physical Interpretations of DIS Structure Function measurements

Some theoretical ideas from the late 1960's...

- Elastic scattering
- The Parton Model (Feynman-Bjorken)
- Theoretical basis of the parton picture
- QCD-improved parton model

First consider the high-energy limit $s \to \infty$ for elastic scattering $e^- p \to e^- p$

The cross section falls rapidly as a function of momentum transfer Q^2, in a manner that is given by the photon propagator **squared** and the square of the Fourier transform of the proton charge distribution.

That Fourier transform falls rapidly with momentum transfer because the proton is an extended object: its charge distribution is spread over a region of $\sim 1\,\mathrm{fm}$.

Another way to look at this is that if one transfers a large momentum to one point in the proton, or to one constituent of it, the other constituents will continue in their original direction, leaving very little wave function overlap probability to produce a single proton in the final state. The same would be true for $e^- p \to e^- p^*$, where p^* is any particular nucleon **resonance.**

The Parton Model (Feynman, Bjorken)

Elastic scattering from point-like constituents predicts that the inclusive cross section $e^- p \to e^- X$ falls only like the Q^{-4} that comes from the square of the photon propagator in the *Bjorken limit* defined by

$$Q^2 \to \infty \text{ at fixed } x = Q^2/(2p\cdot q)\,.$$

The cross section $d\sigma/dQ^2$ has the same dimension as Q^{-4}, so the dimensionless structure functions F_1, F_2, and F_3 approach constants, i.e., functions of x only, in the Bj limit.

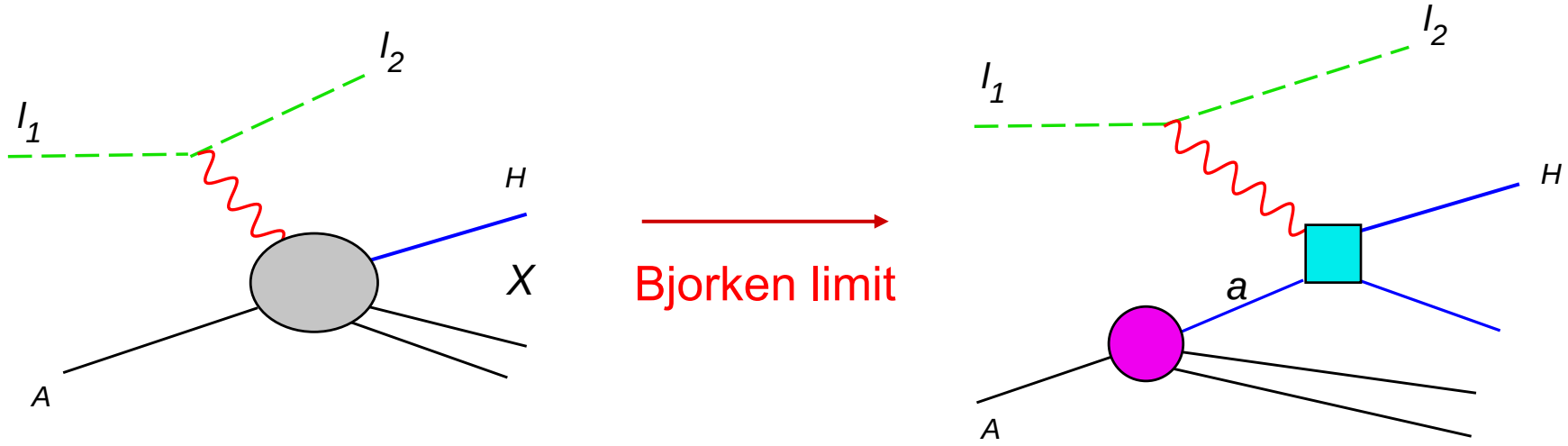

Historical Note

I had the good luck to be a postdoc at SLAC 1968-1970 when the partons were being discovered.

Bjorken's derivation of his scaling law was based on arcane theoretical constructs of the time such as Current Algebra. I suspect I didn't really understand it at the time; and I've certainly forgotten it since. Feynman's point-like constituent view was and remains much more intuitive.

When the scaling functions were found to obey the *Callan-Gross* relation $F_2(x) = 2\,F_1(x)$ that follows from Leading Order scattering from Spin 1/2, the "partons" became clearly identifiable as quarks.

Meanwhile, for all the progress in *Perturbative* QCD since that era, the relationship between the fundamental quarks of QCD and the "constituent" quarks that still guide hadron spectroscopy remains unclear.

$e^- p \to e^- p$ has 3 kinematic variables: E, E', θ; or s, Q^2, x.

E

E', θ

Single photon exchange + Lorentz invariance yields functions of 2 variables:

$$\frac{d^2\sigma}{dx\,dQ^2} = \frac{4\,\pi\,\alpha^2_{\rm EM}}{Q^4}\left[y^2\,F_1 + (1-y)F_2/x\right]$$

Parton model scaling further reduces to functions of 1 variable

$$F_1(x,Q^2) \approx F_1(x) \qquad F_2(x,Q^2) \approx F_2(x)$$

Spin 1/2 partons (quarks) reduces to $F_2 = 2\,x\,F_1$

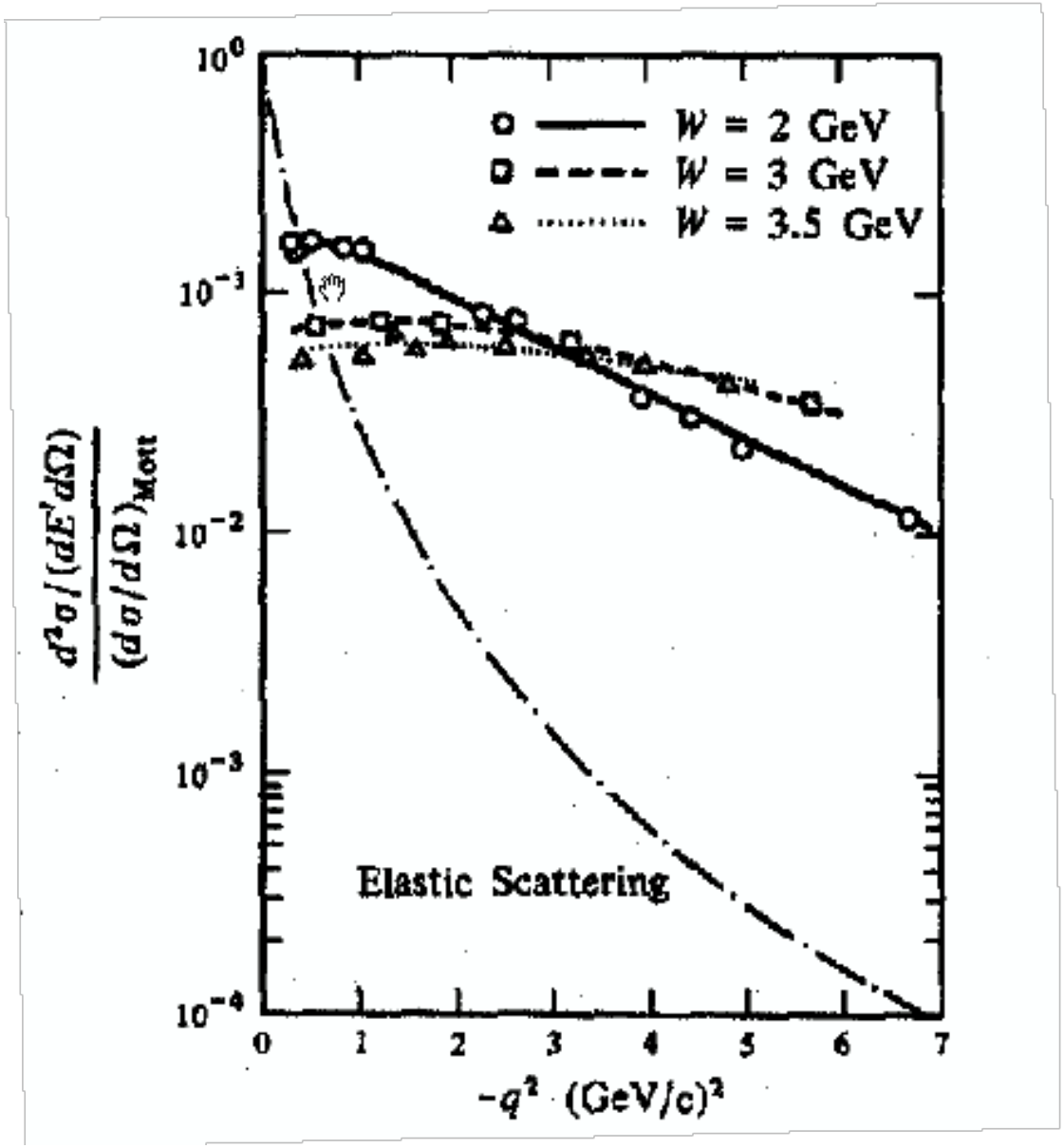

Slow fall-off with Q suggest scattering from point-like constituents.

Early SLAC-MIT data from H. Kendall Nobel prize talk

.Scaling:

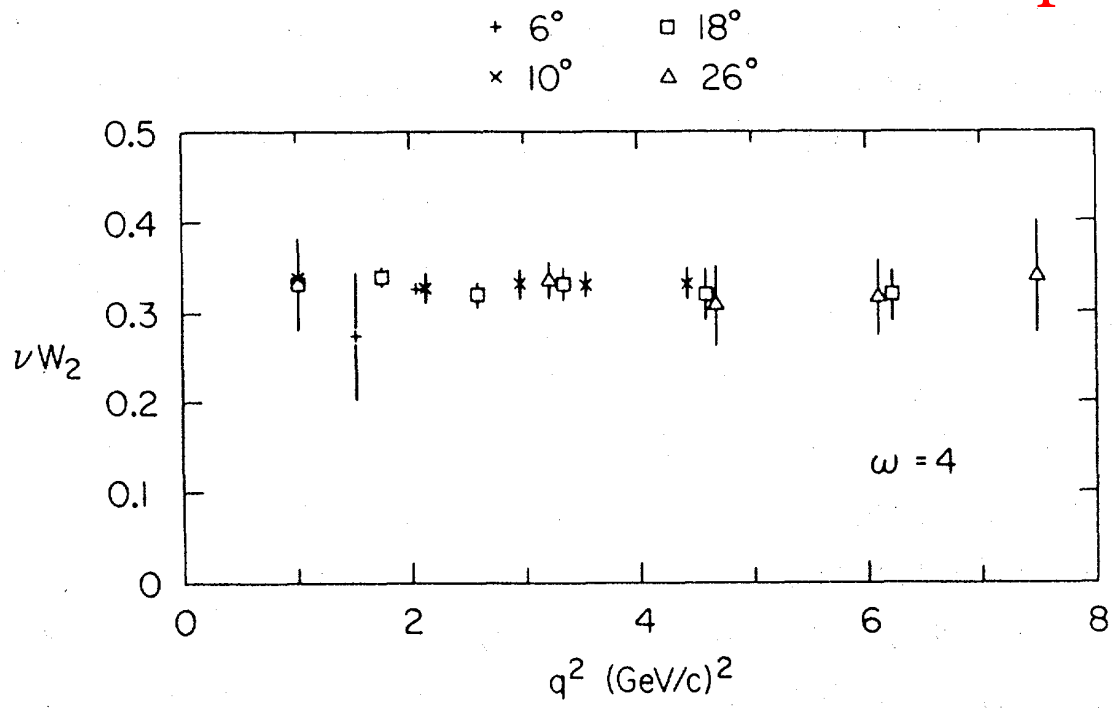

Translations: $\nu\, W_2 \rightarrow F_2, \omega \rightarrow 1/x, q^2 \rightarrow Q^2$.

.Spin 1/2:

?? $\dfrac{xF_2}{F_1} - 1$

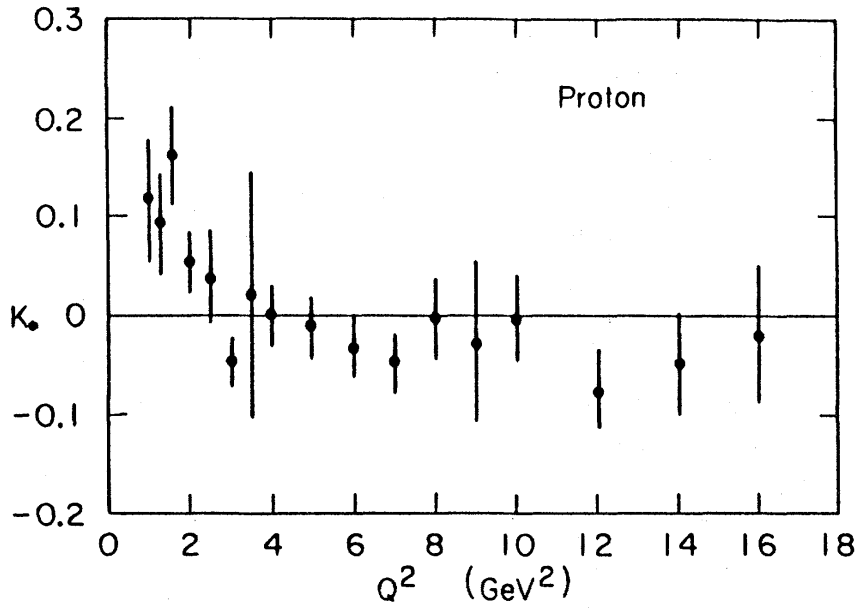

Verification of QPM: fractional electric charge

- Using different probes (e, nu) in DIS processes: can probe electric charge of the partons

  proton: uud

  neutron: ddu

$$F_2(x) = \sum_i e_i^2 x[q_i(x) + \bar{q}_i(x)]$$

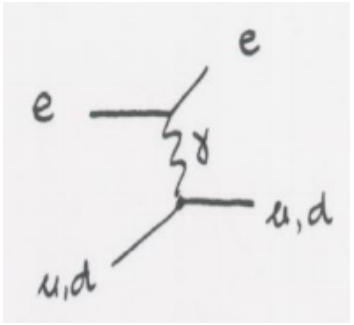

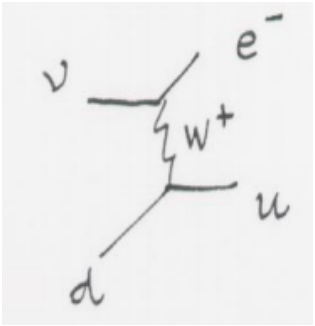

Neutrinos:

- interact only weakly
- left handed particles

$$\begin{aligned} F_2^{ep}(x) &= x[e_u^2(u+\bar{u}) + e_d^2(d+\bar{d})] \\ F_2^{en}(x) &= x[e_u^2(d+\bar{d}) + e_d^2(u+\bar{u})] \\ F_2^{eN}(x) &= \frac{1}{2}(F_2^{ep} + F_2^{en}) \\ &= x\frac{e_u^2 + e_d^2}{2}[u+\bar{u}+d+\bar{d}] \end{aligned}$$

$$\begin{aligned} F_2^{\nu p}(x) &= 2x[d+\bar{u}] \\ F_2^{\nu n}(x) &= 2x[u+\bar{d}] \\ F_2^{\nu N}(x) &= \frac{1}{2}(F_2^{\nu p} + F_2^{\nu n}) \\ &= x[u+\bar{u}+d+\bar{d}] \end{aligned}$$

Confirmed by experimental measurements

$$\frac{F_2^{eN}}{F_2^{\nu N}} = \frac{1}{2}(e_u^2 + e_d^2) = \frac{5}{18} = 0.28 \quad \longleftrightarrow \quad \frac{\mathrm{SLAC}\,eN}{\mathrm{GGM}\,\nu N} = 0.29 \pm 0.05$$

Verification of QPM: fractional electric charge

- Using different probes (e, n… s
  - proton: uud
  - neutron: ddu

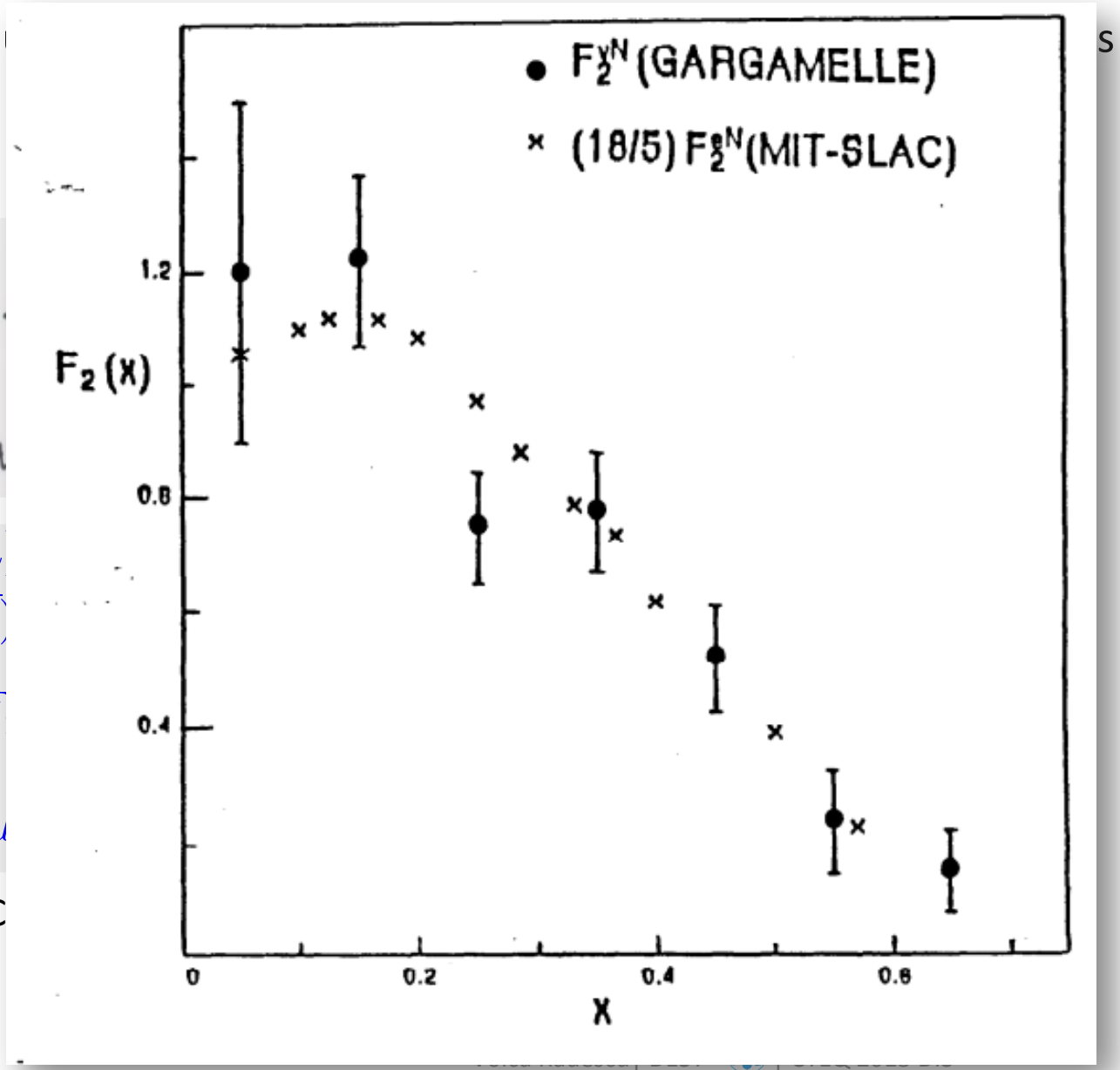

$$F_2^{ep}(x) = x[e_u^2(u+\bar{u}$$
$$F_2^{en}(x) = x[e_u^2(d+\bar{d}$$
$$F_2^{eN}(x) = \frac{1}{2}(F_2^{ep}+F$$
$$= x\frac{e_u^2+e_d^2}{2}[u$$

C

$$\frac{F_2^{eN}}{F_2^{\nu N}} = \frac{1}{2}(e_u^2+e_d^2) = \frac{5}{18}$$

Verification of QPM: valence, sea quarks

- Partons: valence and sea $u = u_{val} + u_{sea}; \quad u_{sea} = \bar{u}$
  $d = d_{val} + d_{sea}; \quad d_{sea} = \bar{d} = \bar{u}$

  - Gross-LLewellyn-Smith sum rule: counting the net number of quarks in the nucleons

$$xF_3^{\nu p} = 2x(d - \bar{d}) = 2xd_v$$
$$xF_3^{\nu n} = 2x(u - \bar{u}) = 2xu_v$$

$$\int_0^1 xF_3^{\nu N}\frac{dx}{x} = \int_0^1 (u_v + d_v)dx$$

QPM predicts that GLS=3; experimental findings agree within errors (Gargamelle).

Verification of QPM: quarks, gluons

The first experimental evidence for gluons was the observation that quarks + antiquarks carry only about half of the proton's momentum in the infinite momentum frame:

$$\sum_i \int_0^1 [q_i(x) + \bar{q}_i(x)]\, x\, dx + \int_0^1 g(x)\, x\, dx = 1$$

Neutrino experiments in the Gargamelle bubble chamber showed that the $q + \bar{q}$ contribution was only 0.49 ± 0.07.

Later we had direct evidence of quarks and gluons in the form of 2-jet and 3-jet events in e^+e^- annihilations:

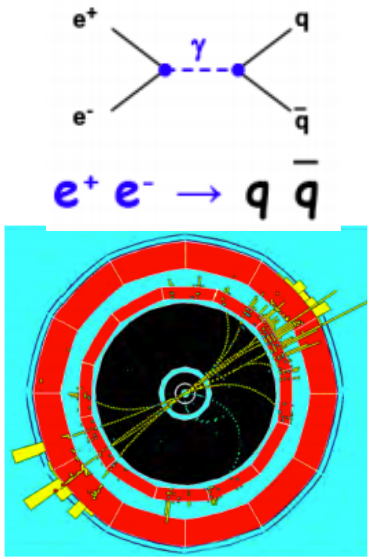

3 jets discovered at DESY in 1979

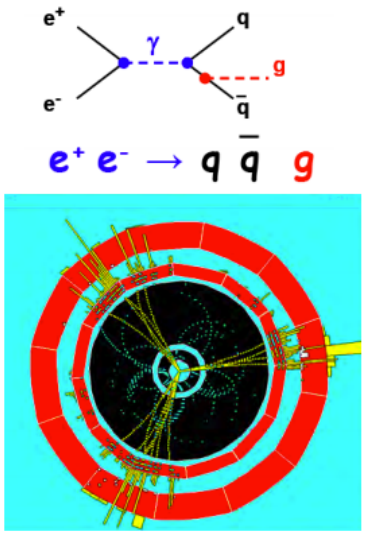

Early SLAC data showed Scaling Violation at other values of x

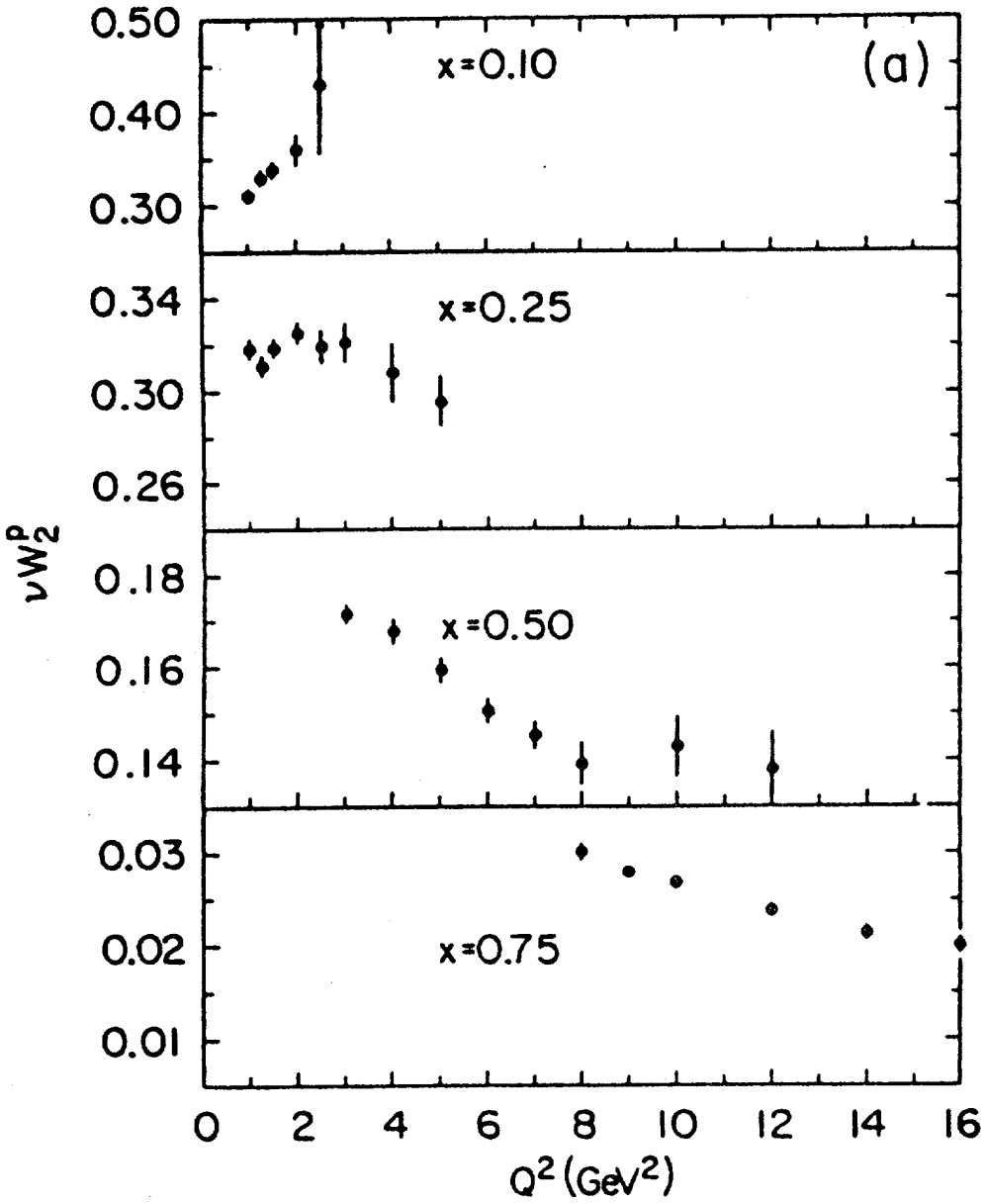

More precise data (Blazey review hep-ex0011078)

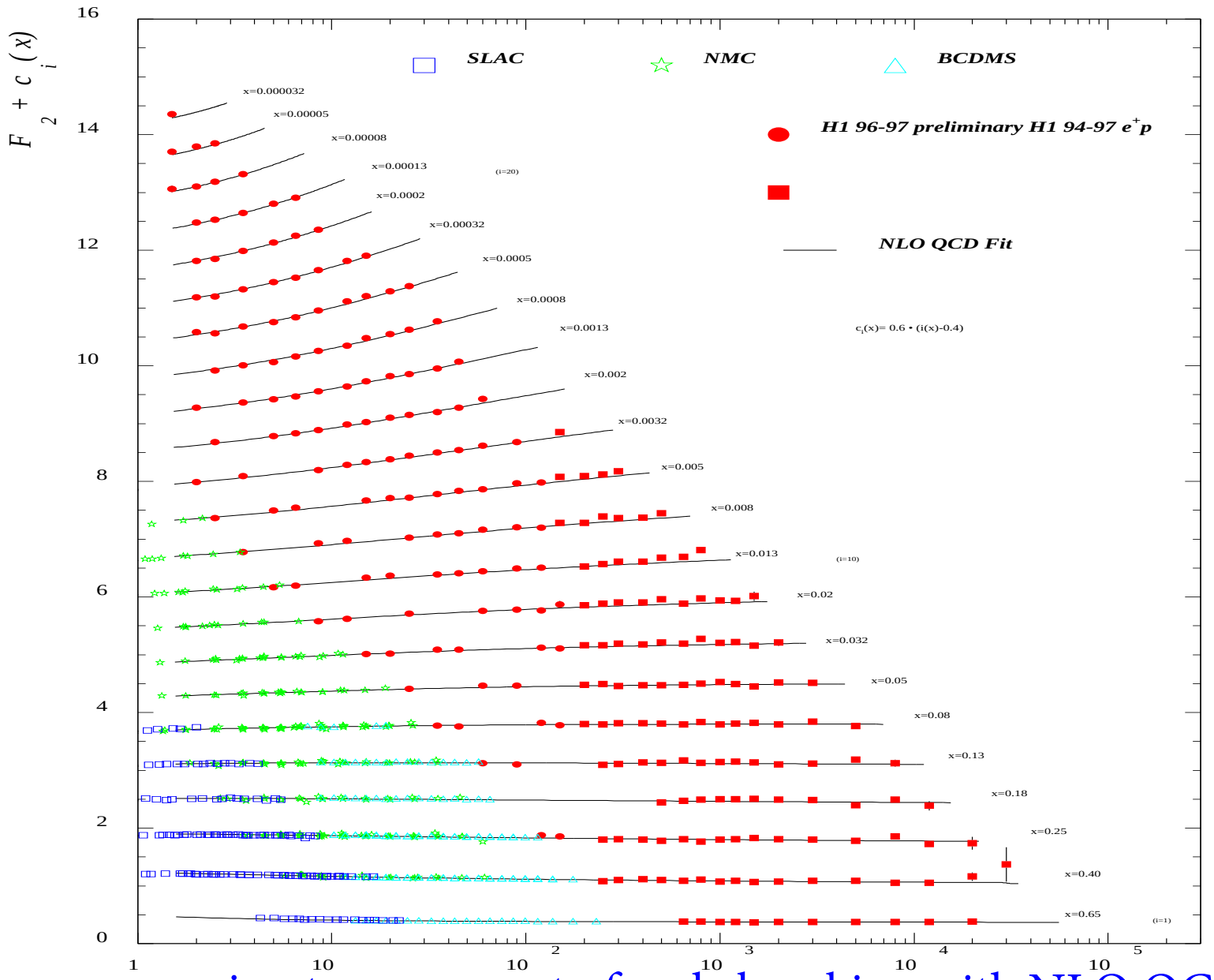

Shows approximate agreement of scale breaking with NLO QCD.

The slow (Log(Q)) breaking of scaling is a natural consequence of QCD

At higher orders in perturbation theory, the quark that is struck by the virtual photon may have come from a "splitting" of parton in the original proton:

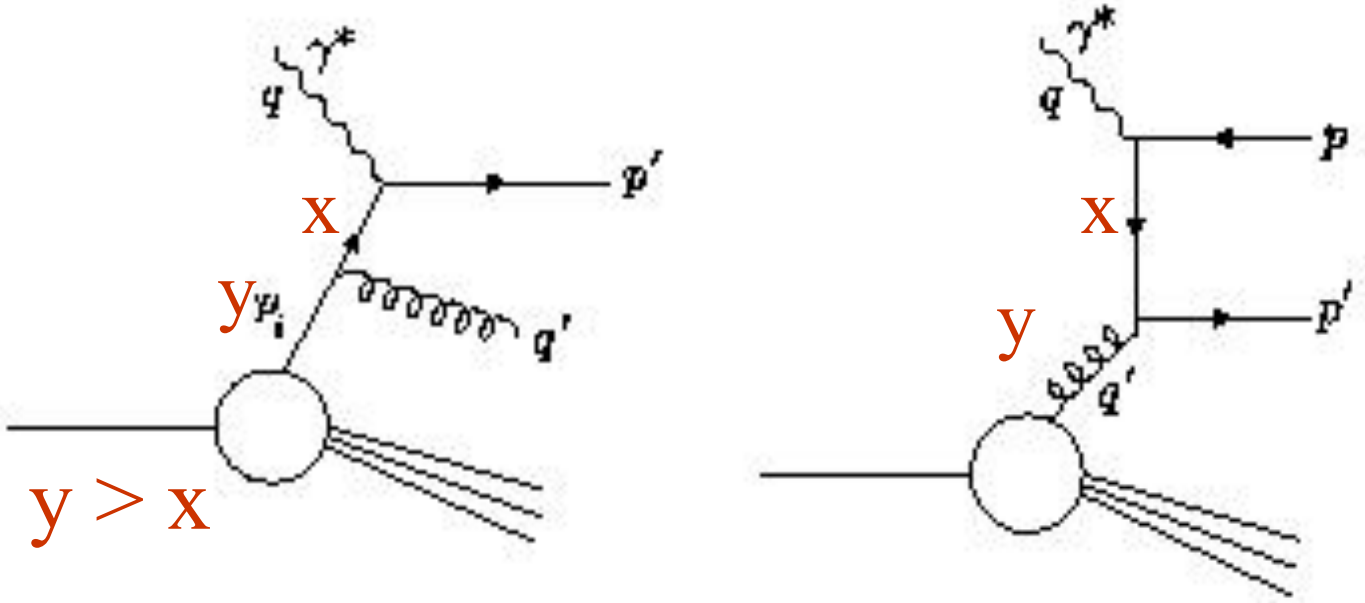

At larger Q, you probe smaller distances and see more splitting. Hence as Q increases, PDFs get larger at small x and smaller at large x.

You can think of the parton distribution functions as evolving with increasing Q through a series of branching processes. The evolution can be computed perturbatively, because the strong coupling alpha_s is sufficiently small (asymptotic freedom) at large Q.

The starting point for this evolution, at a scale of order 1 GeV in Q, cannot be calculated at present because we don't know how to solve QCD in a region where perturbation theory doesn't work.

DGLAP Evolution of the parton distribution functions

$$\frac{d}{d\log\mu_F} f_{a/h}(x,\mu_F) =$$

$$\sum_b \int_x^1 \frac{d\xi}{\xi}\; P_{ab}(x/\xi, \alpha_s(\mu_F))\; f_{b/h}(\xi,\mu_F)$$

$$P_{ab}(x/\xi,\alpha_s(\mu_F)) = P_{ab}^{(1)}(x/\xi)\;\frac{\alpha_s(\mu_F)}{\pi} + P_{ab}^{(2)}(x/\xi)\;\left(\frac{\alpha_s(\mu_F)}{\pi}\right)^2 + \cdots$$

Scaling violation predicted by QCD

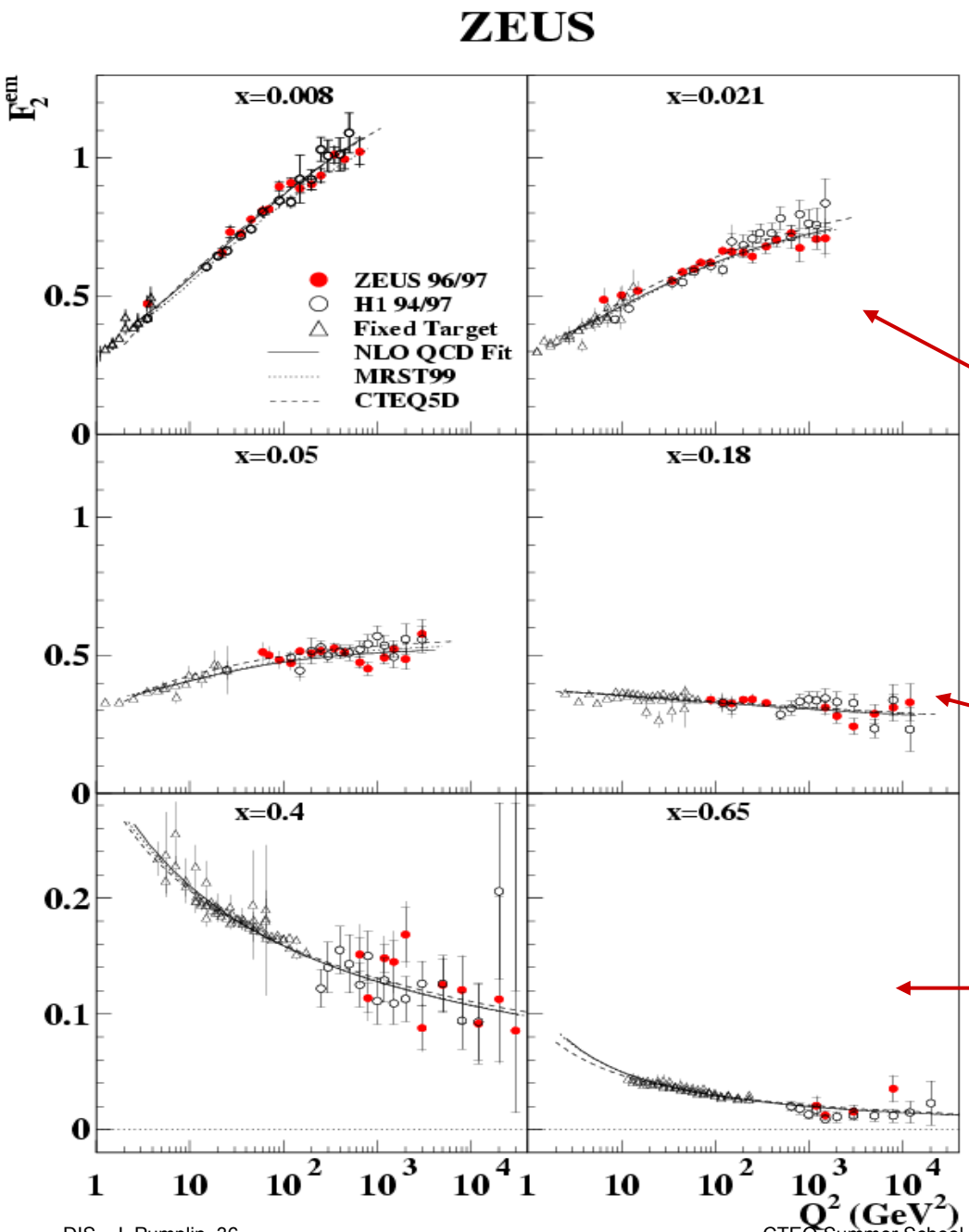

Rise with increasing Q at small-x

Flat behavior at medium x

decrease with increasing Q at high x

For completeness, note that there can also be additional electromagnetic corrections -- e.g. photons radiated from the electron. Published DIS data are usually reported after experts have corrected for these higher-order electromagnetic contributions, so users of DIS data don't have to worry about this.

On the other hand, a photon can play a role as one of the partons. This is of course suppressed by the small alpha_EM; but it can nevertheless be significant in some processes at LHC. Specialized parton distributions in which some of the proton momentum is carried by photon are already available.

What DIS experiments are used for PDFs fits?

The HERA Collider

The first and only ep collider in the world

Located in Hamburg

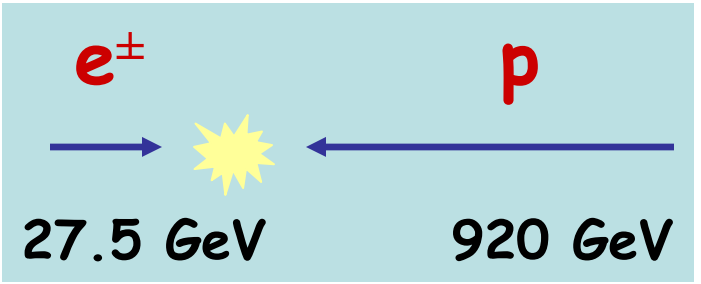

$\sqrt{s}$ = 318 GeV

Equivalent to fixed target experiment with 50 TeV $e^{\pm}$

Two independent storage rings

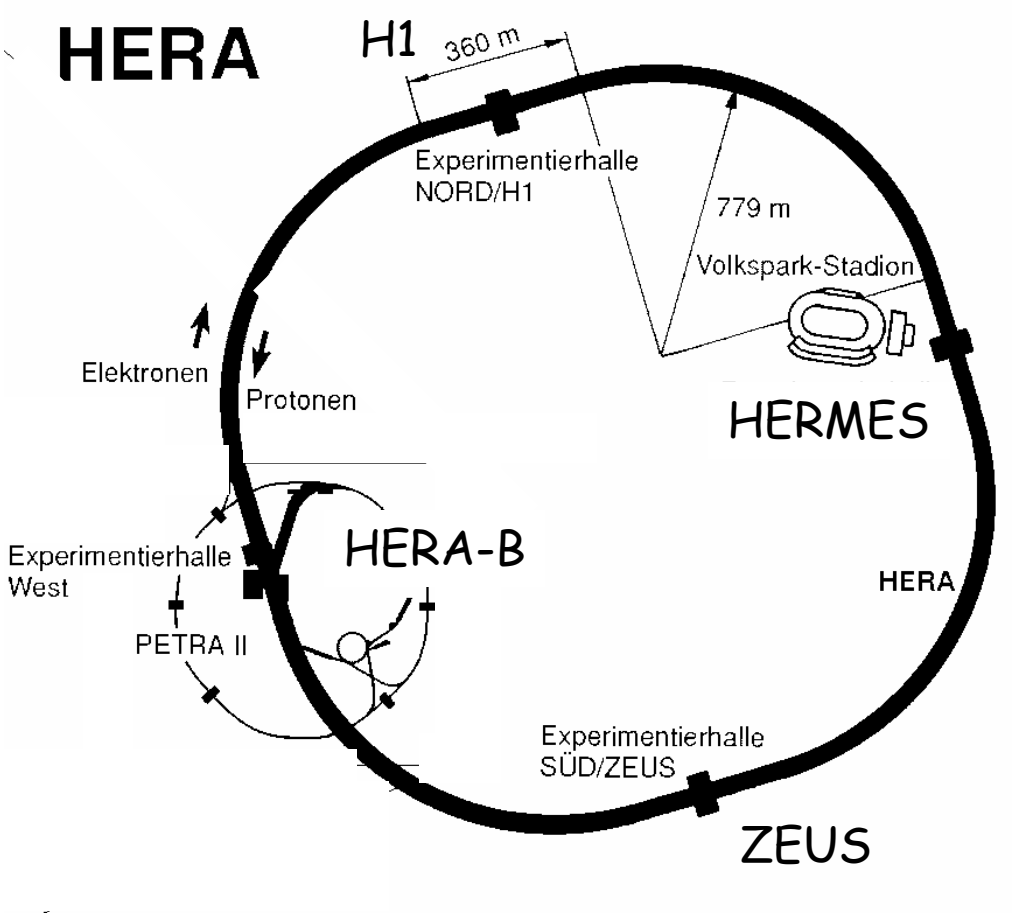

H1 – ZEUS

Colliding beam experiments

HERA-B

Uses p beam on wire target
Goal: B - physics

HERMES

Uses $e^{\pm}$ beam on gas jet target
Both lepton and target polarized
Measurement of polarized structure functions

The Collider Experiments

H1 Detector

Complete 4π detector with

Tracking
- **Si-μVTX**
- **Central drift chamber**

Liquid Ar calorimeter

→ $\hat{\imath}E=E = 12\% \oplus \frac{}{E[GeV]}$ (e:m:)

$\hat{\imath}E=E = 50\% \oplus \frac{}{E[GeV]}$ (had)

Rear Pb-scintillator calorimeter

→ $\hat{\imath}E=E = 7{:}5\% \oplus \frac{}{E[GeV]}$ (e:m:)

μ chambers

and much more…

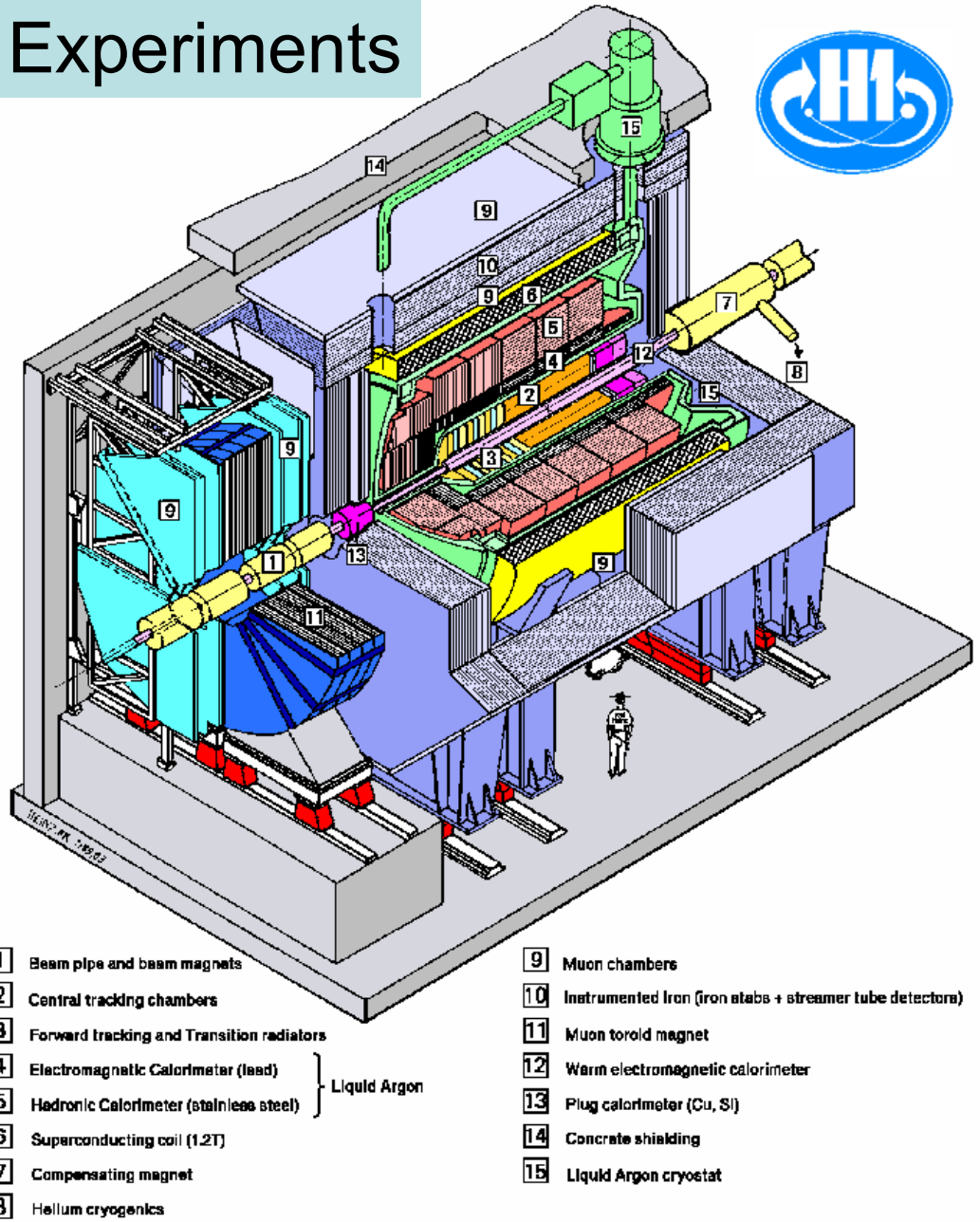

ZEUS Detector

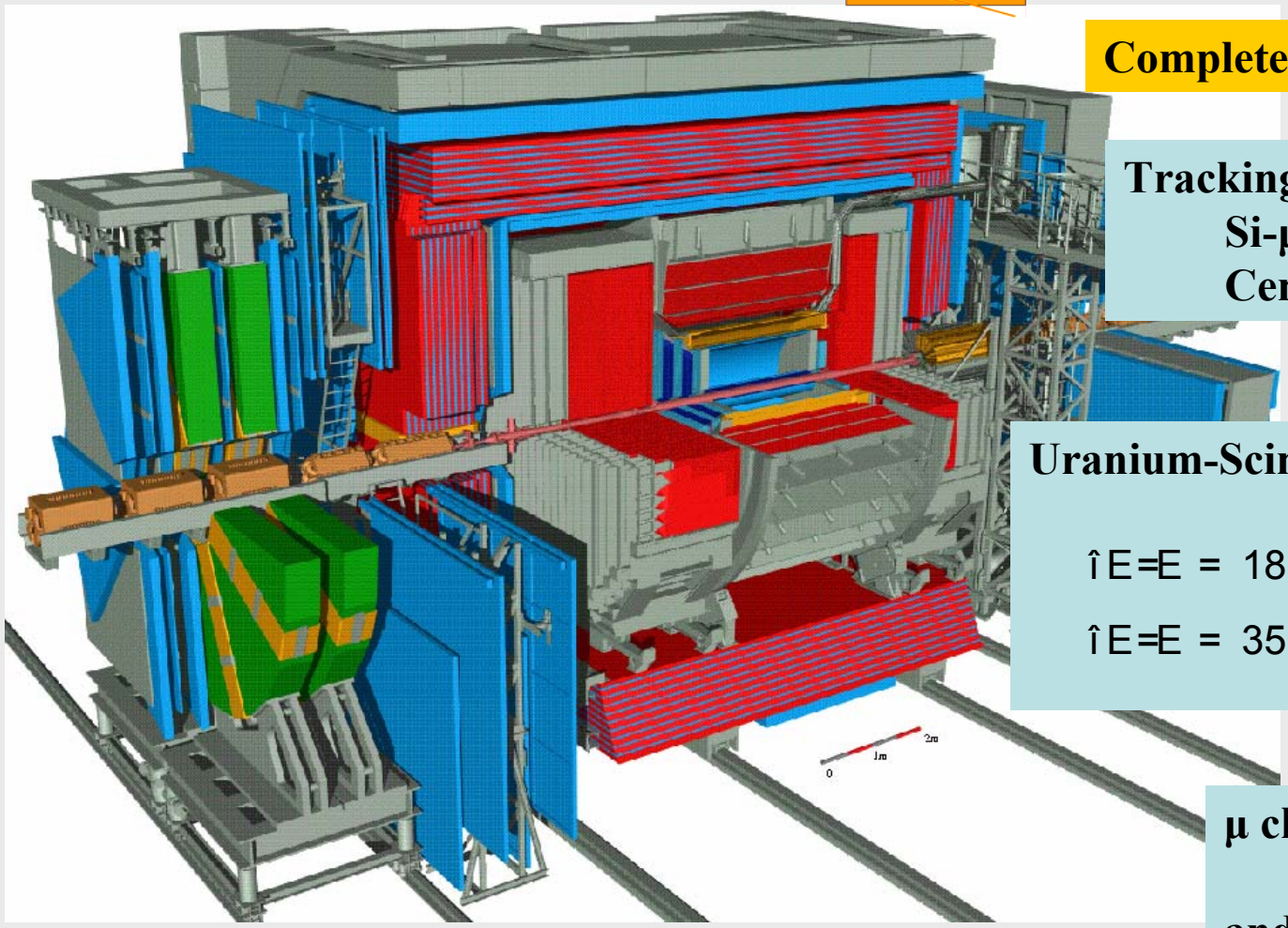

Complete 4π detector with

Tracking
- **Si-μVTX**
- **Central drift chamber**

Uranium-Scintillator calorimeter

$$\hat{\imath}E/E = 18\%/\sqrt{E[\mathrm{GeV}]}\ (\mathrm{e.m.})$$

$$\hat{\imath}E/E = 35\%/\sqrt{E[\mathrm{GeV}]}\ (\mathrm{had})$$

μ chambers

and much more…

Both detectors asymmetric

NC and CC incl. Processes measured at HERA

$$\text{NC}: \quad e^{\pm} + p \to e^{\pm} + X, \qquad \text{CC}: \quad e^{\pm} + p \to \bar{\nu}_e(\nu_e) + X$$

NC:

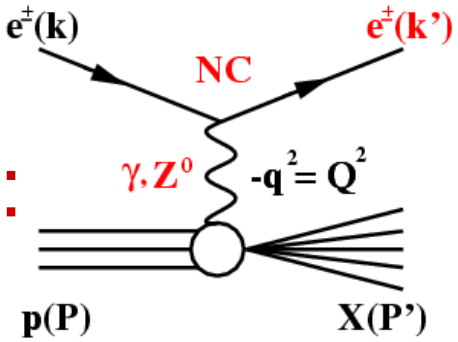

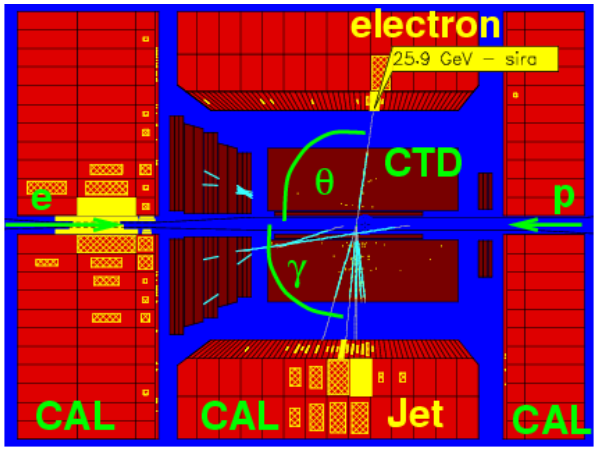

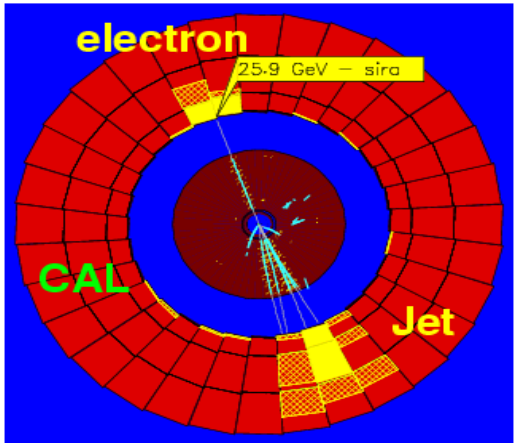

CC:

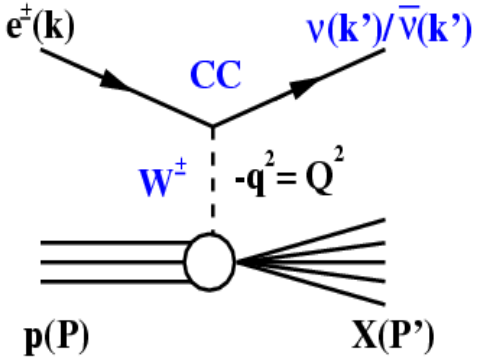

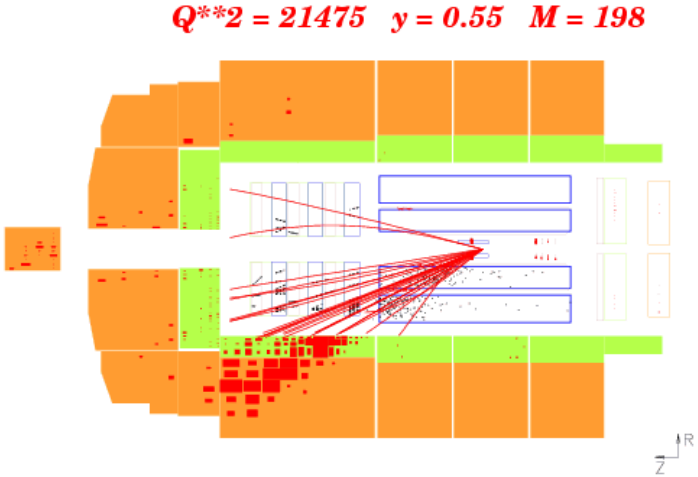

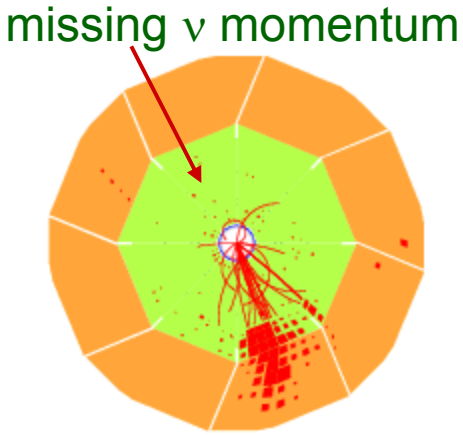

Measurement of $F^{\gamma}_2(x,Q^2)$

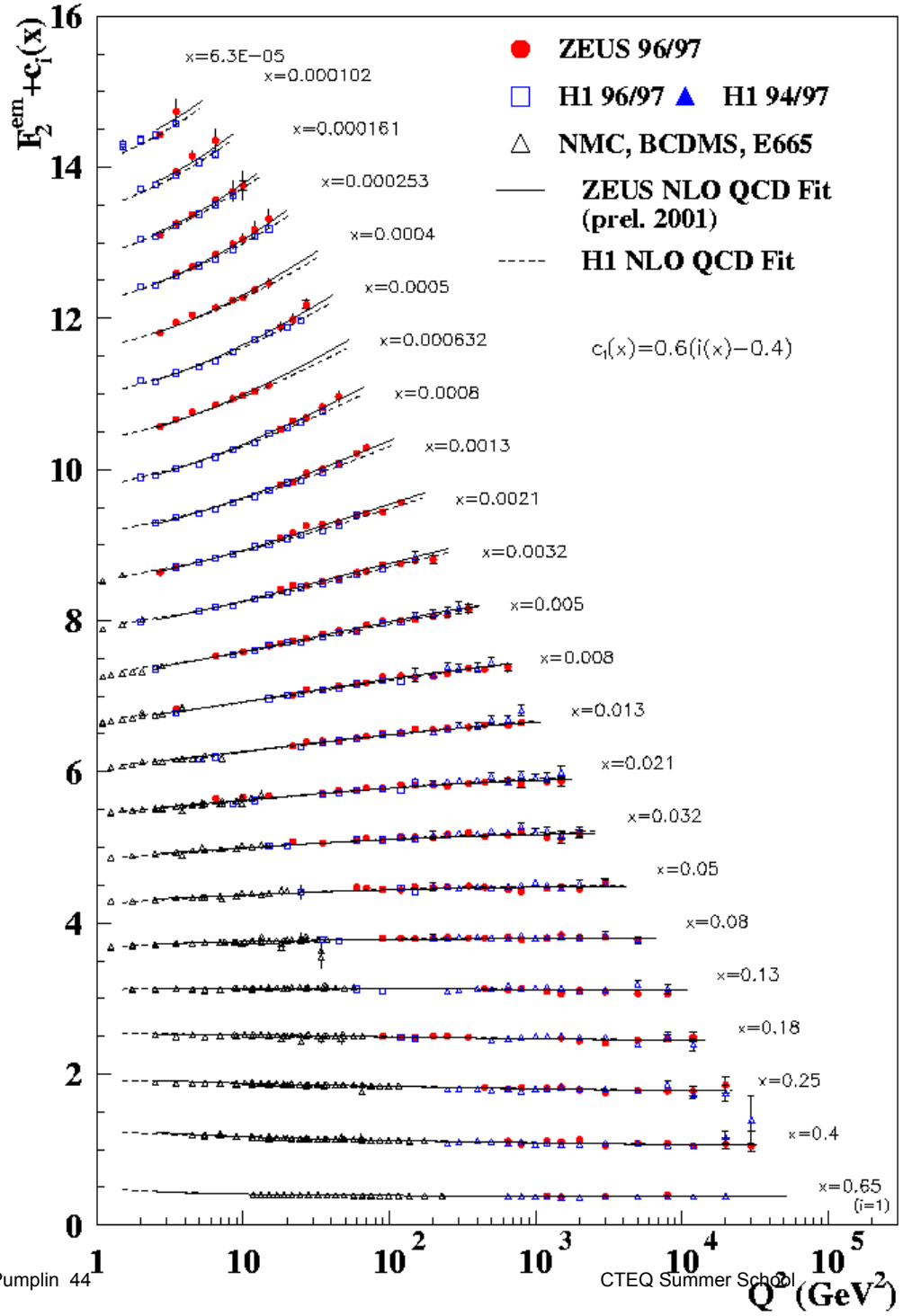

Measurement precision is at the few percent level.

A great deal of effort has been put into combining the H1 and Zeus results to reduce systematic errors.

A major finding at Hera: rise of $F_2(x,Q)$ at small x

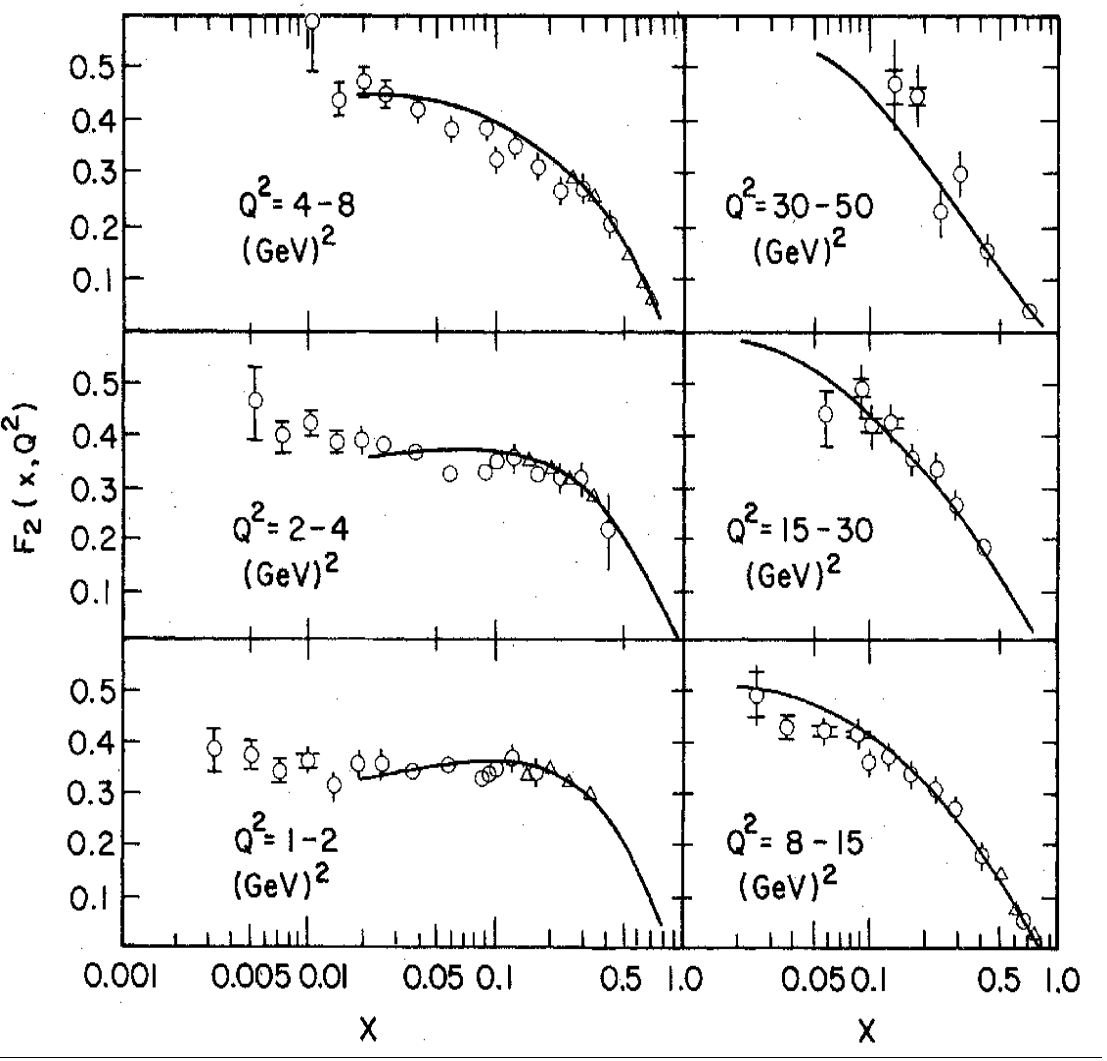

Early fixed-target results:

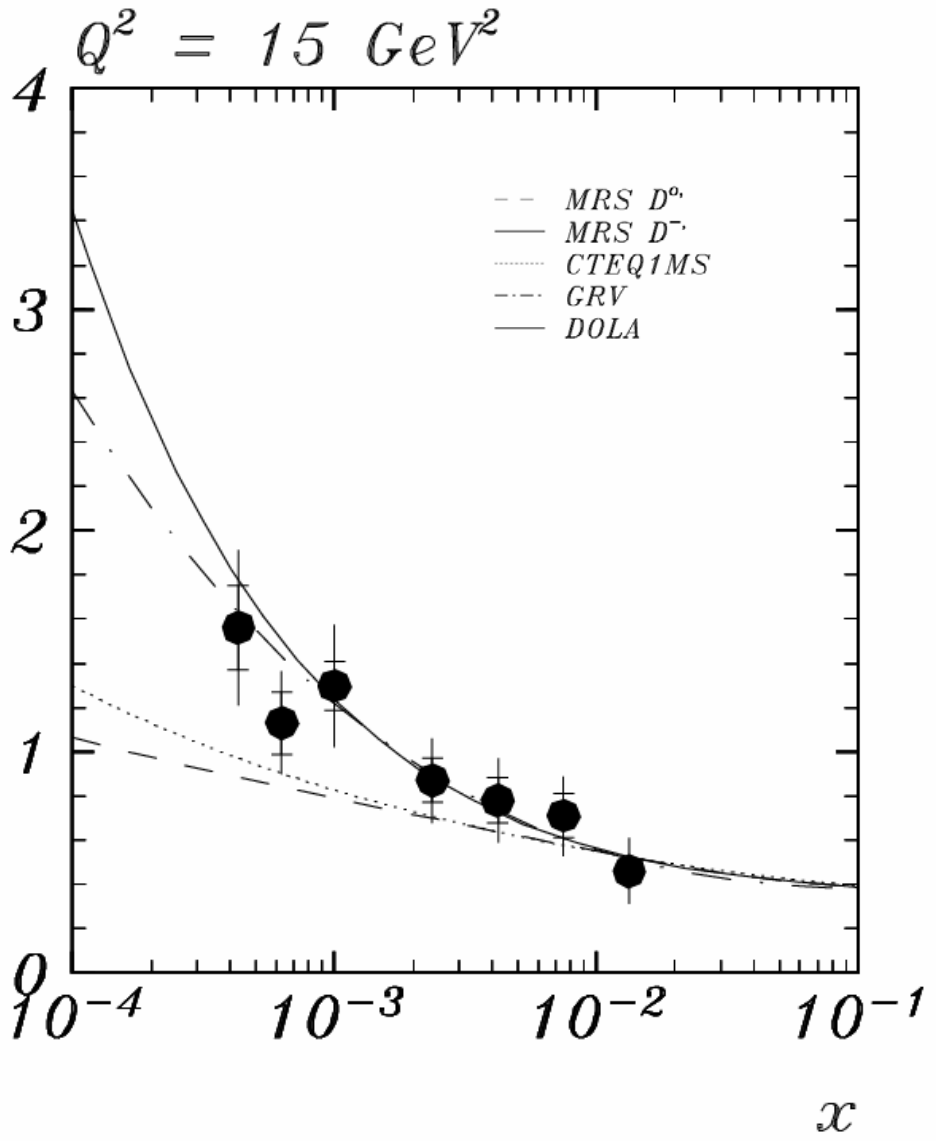

F_2 rise towards low-x established with ~20 nb^{-1} in early Hera run

Comparing NC and CC Xsec's at HERA: EW Unification

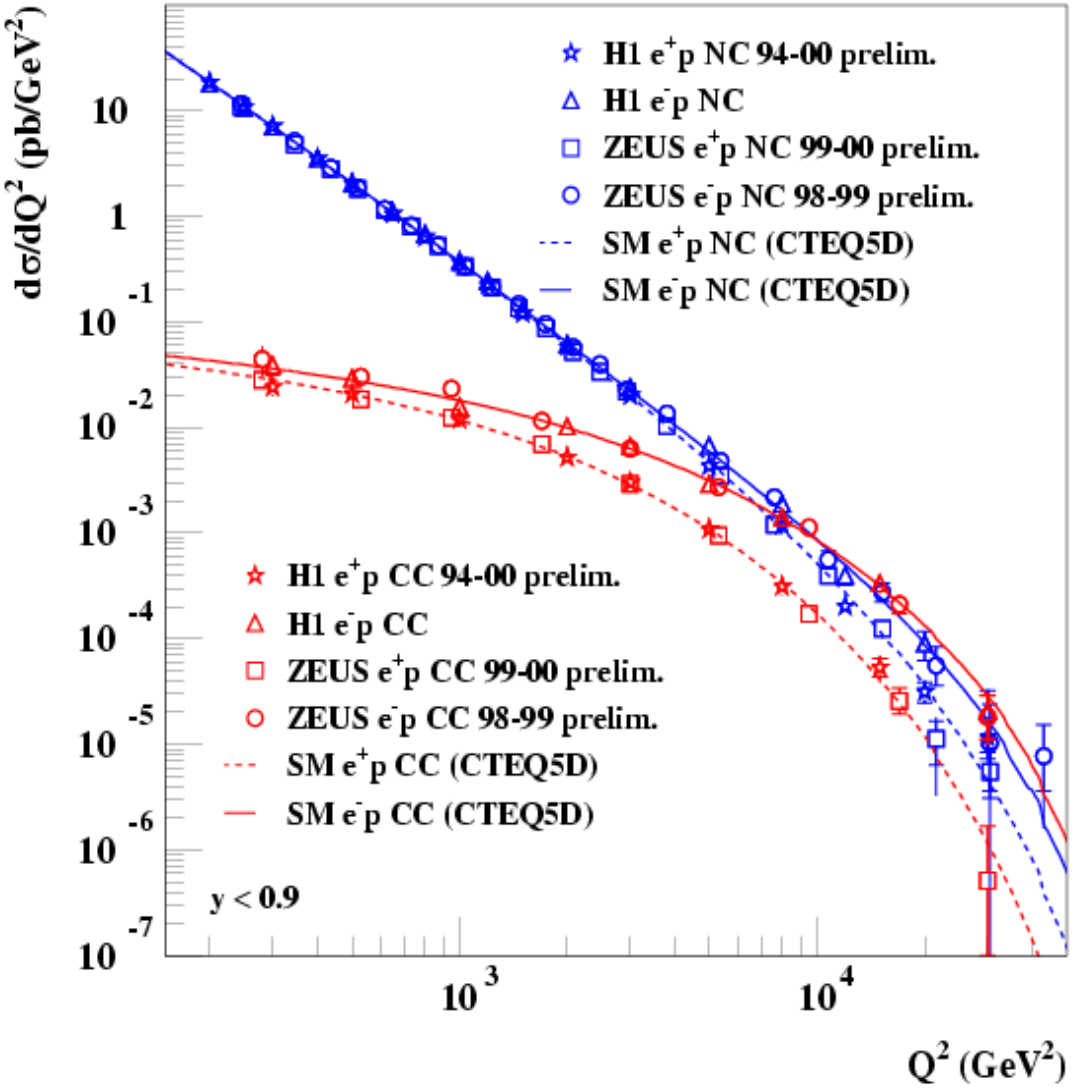

NC cross section sharply decreases with decreasing Q^2 (dominant γ exchange): $\sim 1/Q^4$

CC cross section approaches a constant at low Q^2 $\sim[M^2_W/(Q^2+M^2_W)]^2$

Dramatic confirmation of the unification of electromagnetic and weak interactions in the SM.

HERA (H1,Zeus): 27.5 GeV $e^{\pm}$ on 920 GeV p: $\sqrt{s} = 318$GeV

- Precise $e^{\pm}p \to e^{\pm}X$ data over wide kinematic range a major input to **all** PDF fits.

- Dominant contribution to $e^{\pm}\,p \;\to e^{\pm}\,X$ is from photon exchange, so cross sections is proportional to quark charge squared. Hence gives strongest information on partons with charge $\pm 2/3$: dominantly u ($+\,\bar{u}$, c, $\bar{c}$ with no differentiation between them); less information on partons with charge $\pm 1/3$: dominantly d ($+\,\bar{d}$, s, $\bar{s}$, b, $\bar{b}$ with no differentiation between them); and no direct information on the gluon distrbution. Nevertheless, the variation of $f_{a\in p}(x,\mu)$ with μ can be calculated in QCD perturbation theory ("DGLAP evolution"), which helps to determine the gluon

  .

- At very large momentum transfer, Z^0 exchange becomes comparable to γ exchange; which makes the difference between $e^-\,p \;\to\; e^-\,X$ and $e^+\,p \;\to\; e^+\,X$ sensitive to γ/Z^0 interference; the Z^0 exchange contribution provdes additional flavor information.

- The charged-current process $e^{\pm}\,p \;\to \nu\,X$ comes from $W^{\pm}$ exchange, which gives additional information on flavor differentiation.
- F_L measurement.
- HERA accelerator disassembled in June 2007; H1+Zeus combined experimental data analysis expected soon (2014?)

BCDMS, NMC 280GeV μ^+ on proton or deuteron at rest $\sqrt{s}$=22.9GeV

- Large luminosity of fixed-target experiment allows measurements up to large x (e.g. $x > 0.5$).
- Measuring both $\mu^+ p \to \mu^+ X$ and $\mu^+ d \to \mu^+ X$ can be used get DIS on the neutron, if one makes or ignores nuclear binding corrections. The isospin symmetry assumption that u and d distributions in neutron and proton are identical except for $u \leftrightarrow d$, then gives useful information on d and $\bar{d}$
- BCDMS data taken 1978–1985, NMC 1986–1989. Older technology.
- NMC data problematic—can't be fit well.

CDHSW $\sim 20 - 200$GeV ν_μ and $\nu^- \mu$ on iron fixed target. (1976-1984)

- $\nu\,\mathrm{Fe} \rightarrow \mu^- X$ through W^+ exchange and $\bar{\nu}\,\mathrm{Fe} \rightarrow \mu^+ X$ through W^- exchange give useful information to differentiate between quark flavors.

- The data were taken on an iron target **(1200 tons)** to obtain a sufficient event rate. Unfortuately, we don't really know how to correct for nuclear binding effects; so it will be a happy day when LHC data such as inclusive W and Z production can be used instead.

More on neutrino DIS from D. Naples (CTEQ school 2013)

http://www.physics.smu.edu/olness/ftp/misc/cteq/SampleLectures/naples1.pdf

Y-Dependence ν vs. $\overline{\nu}$ Cross Sections

$$\frac{d^2\sigma^{\nu}}{dxdy} = \frac{G^2 sx}{\pi}\left[\mathrm{q(x)} + \overline{\mathrm{q}}\mathrm{(x)}(1-y)^2\right]$$
$$\frac{d^2\sigma^{\overline{\nu}}}{dxdy} = \frac{G^2 sx}{\pi}\left[\overline{\mathrm{q}}\mathrm{(x)} + \mathrm{q(x)}(1-y)^2\right]$$

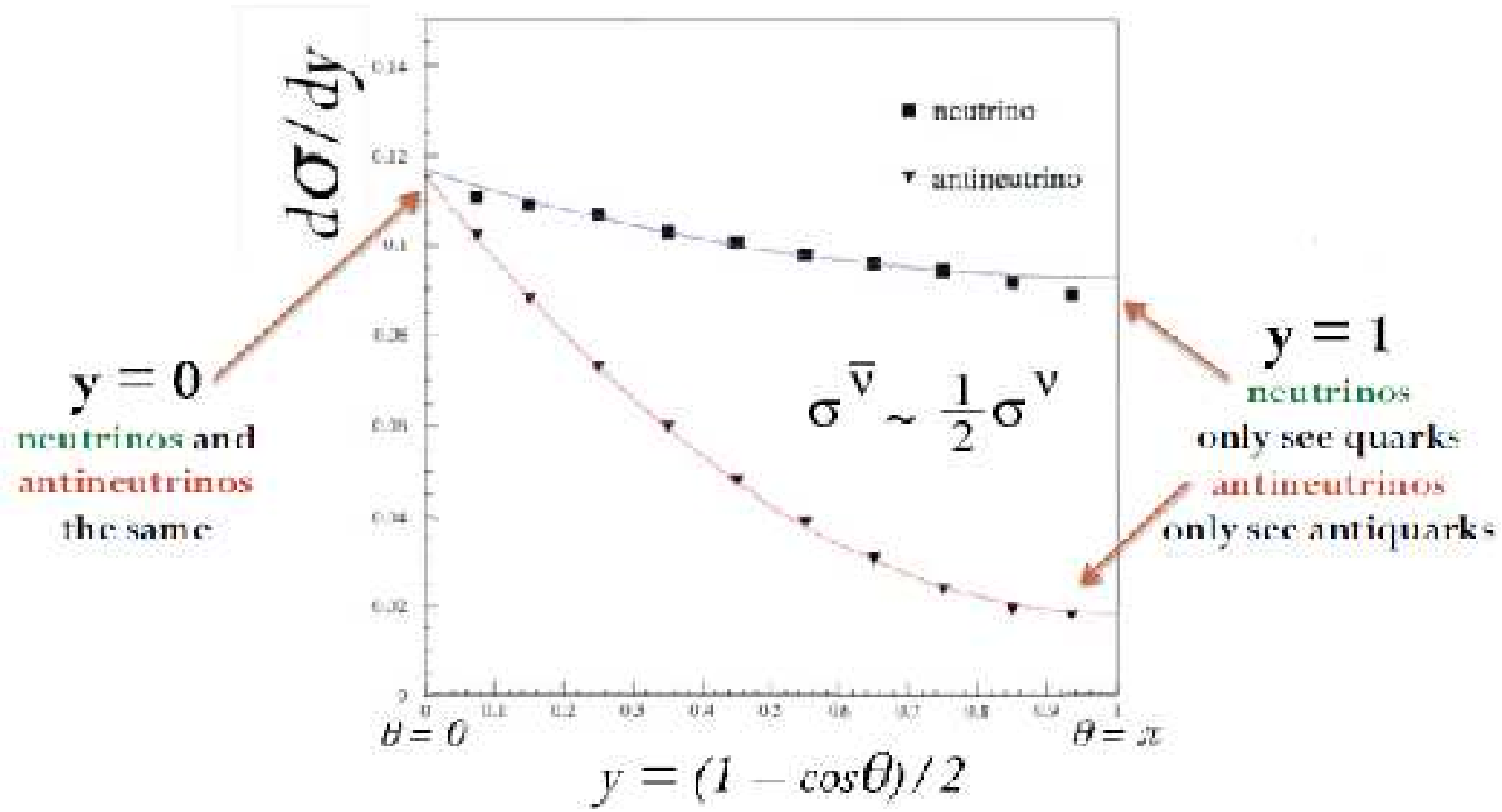

Neutrino SFs in the Parton Model

QPM: scattering off the nucleon is the incoherent sum of elastic scattering off the constituents.

- Assume no spin 0 constituents: Callan-Gross relation (R=0) $F_2(x) = 2xF_1(x)$.
- Relate SFs to PDFs by matching y-dependence in cross section terms.

Neutrino Structure Functions

$$F_2(x) = 2\Sigma x\left(q(x) + \overline{q}(x)\right)$$

$$xF_3(x) = 2\Sigma x\left(q(x) - \overline{q}(x)\right)$$

Flavor sensitivity: lepton number and charge conservation.

ν selects: $d, s, \overline{u}, \overline{c}$ $\quad q^{\nu p}(x) = d^p(x) + s^p(x) \quad \overline{q}^{\nu p}(x) = \overline{u}^p(x) + \overline{c}^p(x)$

$\overline{\nu}$ selects: $u, c, \overline{d}, \overline{s}$ $\quad q^{\overline{\nu} p}(x) = u^p(x) + c^p(x) \quad \overline{q}^{\overline{\nu} p}(x) = \overline{d}^p(x) + \overline{s}^p(x)$

Neutrino Structure Functions

More practical: *isoscalar* target ($N_n = N_p$)

- *(Neutrino experiments use nuclear target/detectors)*.
- Isospin symmetry

$$u(x) \equiv u^p(x) = d^n(x) \quad d(x) \equiv d^p(x) = u^n(x)$$
$$\overline{u}(x) \equiv \overline{u}^p(x) = \overline{d}^n(x) \quad \overline{d}(x) \equiv \overline{d}^p(x) = \overline{u}^n(x)$$

- Assume symmetric heavy quark seas $s = \overline{s}$ and $c = \overline{c}$

$$F_2^{\nu N} = F_2^{\overline{\nu} N} = x\left(u + \overline{u} + d + \overline{d} + 2\overline{s} + 2c\right)$$
$$xF_3^{\nu N} = x\left(u + d - \overline{u} - \overline{d} + 2s - 2\overline{c}\right)$$
$$xF_3^{\overline{\nu} N} = x\left(u + d - \overline{u} - \overline{d} + 2\overline{s} - 2c\right)$$

$F_2^{\nu N}$	all quarks
xF_3	valence quarks
ΔxF_3	$= 4x(s - c)$ heavy quark seas.

Future DIS Experiments

Experiment scheduled for upgraded JLAB

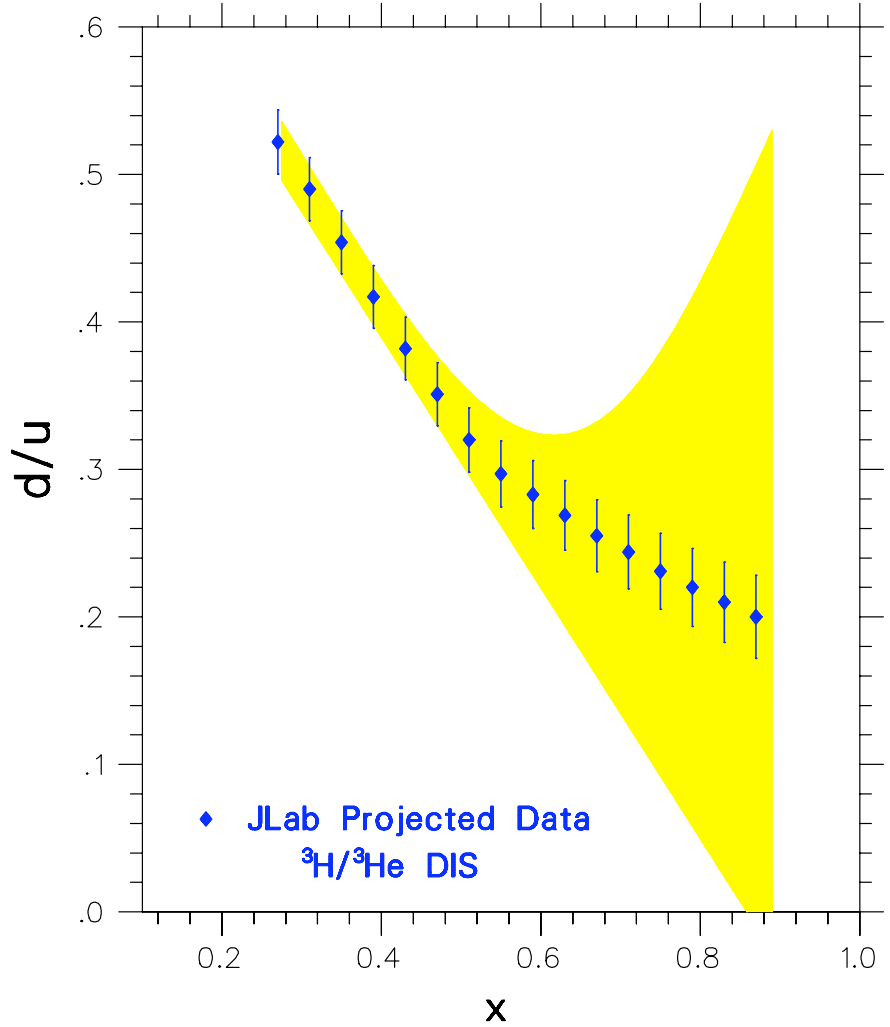

Projected inelastic data ($W^2 > 4$ GeV^2, except for the highest-x point for which $W^2 = 3$ GeV^2) for the d/u quark distribution ratio from the proposed ^{3}H/^{3}He JLab experiment with a 11 GeV electron beam. The error bars include point-to-point statistical, experimental and theoretical uncertainties, and an overall normalization uncertainty added in quadrature. The shaded band indicates the present uncertainty due mainly to possible binding effects in the deuteron.

(But note W^2 > 4 GeV^2, not W^2 > 12.5 GeV^2.)

Future ep collider?

LHeC (ep collider to complement LHC at CERN), EIC

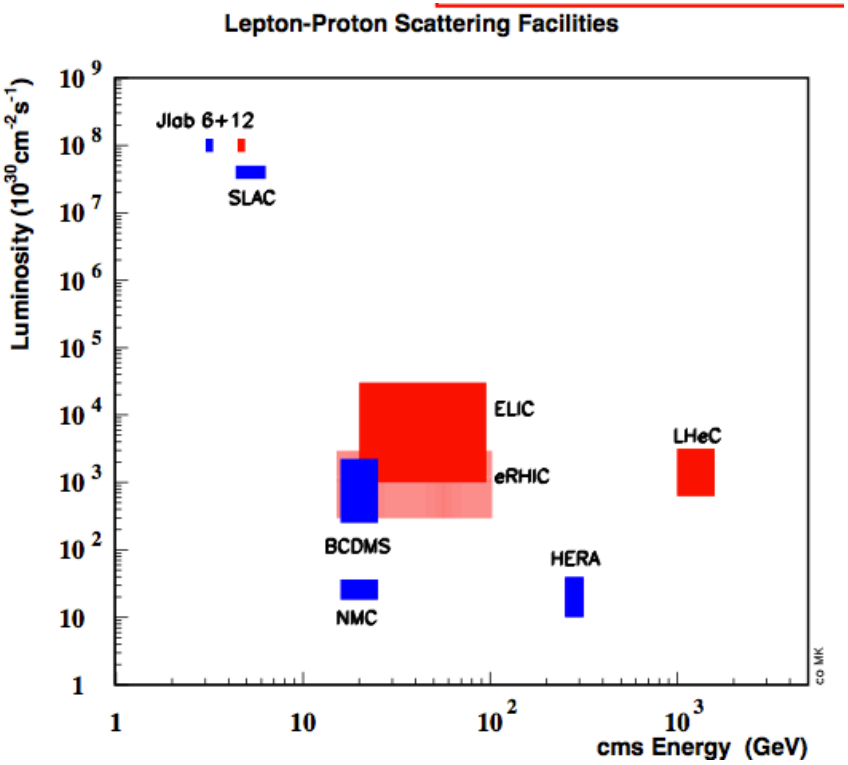

- LHeC sensitivity extends to x=10^{-6}
- Much increased luminosity for EIC and LHeC colliders compared to HERA.

LHeC Kinematic region

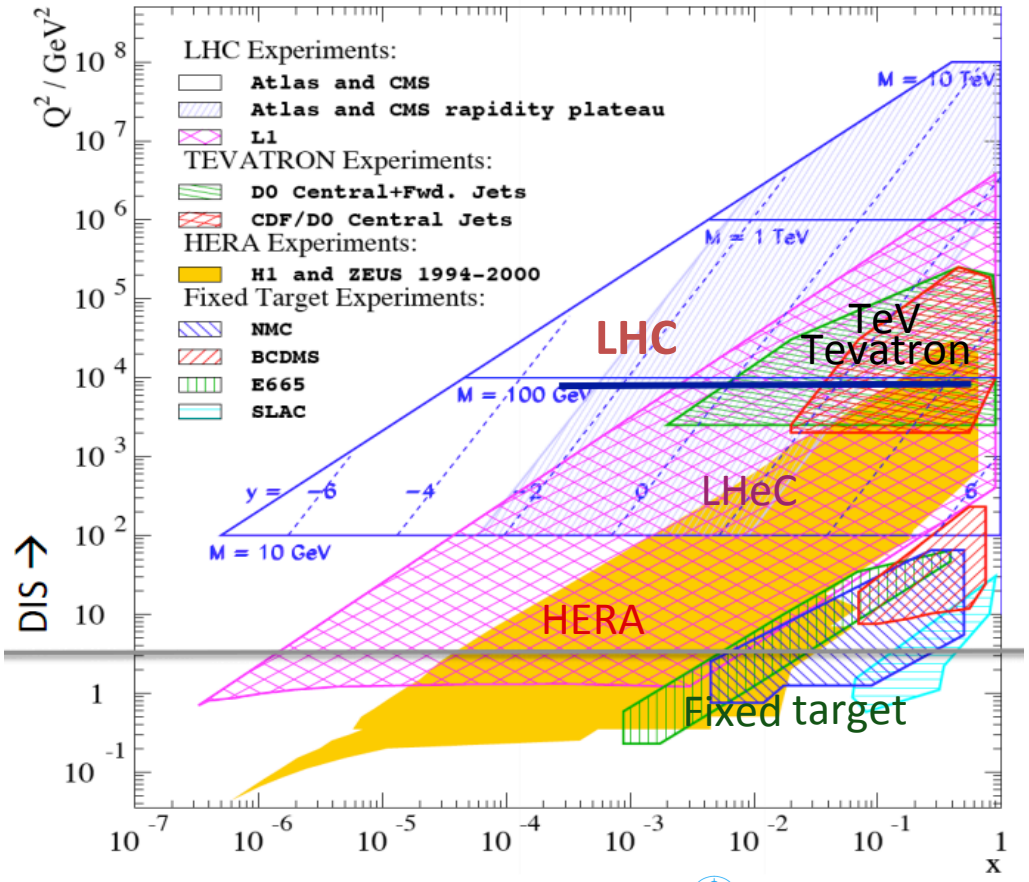

Motivation for LHeC

- What HERA could/did not do:

Test of the isospin symmetry (u-d) with eD	no deuterons
Investigation of the q-g dynamics in nuclei	no time for eA
Verification of saturation prediction at low x	too low c.o.m energy
Measurement of the strange quark distribution	too low Luminosity
Discovery of Higgs in WW fusion in CC	too low cross section
Study of top quark distribution in the proton	too low c.o.m energy
Precise measurement of FL	too short running time with low energy runs
Resolving d/u question at large Bjorken x	too low Luminosity
Determination of gluon distribution at hi/lo x	too small range
High precision measurement of αs	overall not precise enough

HEP needs a TeV energy scale machine with 100 times higher luminosity than HERA to develop DIS physics further and to complement the physics at the LHC. The Large Hadron Collider p and A beams offer a unique opportunity to build a second ep and first eA collider at the energy frontier. (M. Klein)

Excerpts from a previous lecture

Measuring PDFs by QCD fitting

Jon Pumplin

PDF School (DESY 20–23 October 2009)

Hadrons interact at large momentum transfer (=short distance) through their quark and gluon constituents.

Owing to the asymptotic freedom property of QCD, $\alpha_s(\mu)$ is small so most hard pp collisions at the LHC will be described by the interaction of a single quark or gluon from one of the protons with a single quark or gluon from the other.

Hence the subject of this school: we study the PDFs $f_a(x,\mu)$ which describe the "1-body" probability densities for $a = u,\ \bar{u},\ d,\ \bar{d},\ s,\ \bar{s},\ c,\ \bar{c},\ b,\ \bar{b},$ (or γ) with the spin structure and correlations integrated out.

Two points of view

The PDFs are a Necessary Evil — essential phenomenological tools to make perturbative calculations of signals and backgrounds at hadron colliders. It is of essential practical importance to measure the PDFS in order to make use of data from the Tevatron and LHC. Along with this comes the difficult task of assessing the uncertainty range of the answers obtained.

The PDFs are a Fundamental Measurement — an opportunity to interplay with knowledge from the nonperturbative arenas of QCD, e.g.,

- Regge theory
- Lightcone physics
- Lattice gauge

The PDFs $f_a(x, \mu)$ for each flavor a are functions of two variables:

- x = light-cone momentum fraction
- μ = QCD factorization scale ($\approx 1/\text{distance}$), typically Q for DIS; E_T or $E_T/2$ for inclusive jet production.

The evolution in μ is computable at NLO or NNLO by the QCD renormalization group DGLAP equations. Hence the problem of determining the PDFs reduces to a problem of determining the x dependence for each flavor at a chosen small scale μ_0 (e.g. ~ 1.4 GeV).

Theoretical basis for PDF fitting

- Factorization Theorem – Short distance and long distance are separable, and PDFs are "universal," i.e., process independent.

- Asymptotic Freedom – Hard scattering is weak at short distance, and hence perturbatively calculable.

- DGLAP Evolution – Evolution in μ is perturbatively calculable, so the functions to be determined depend only on x.

Factorization Theorem

$$F_A^\lambda(x, \frac{m}{Q}, \frac{M}{Q}) = \sum_a f_A^a(x, \frac{m}{\mu}) \otimes \hat{F}_a^\lambda(x, \frac{Q}{\mu}, \frac{M}{Q}) + \mathcal{O}((\frac{\Lambda}{Q})^2)$$

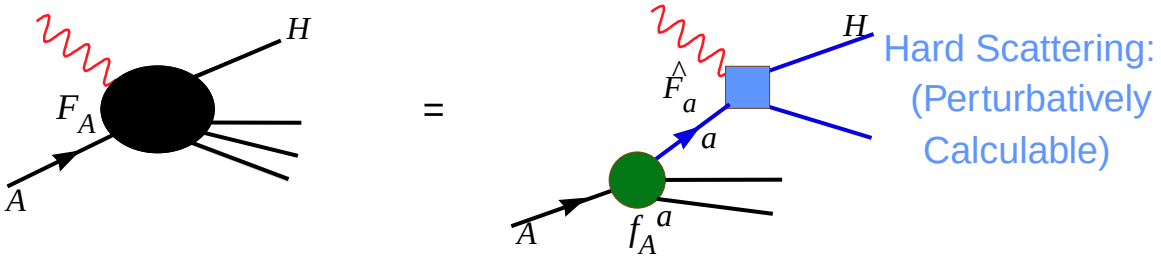

Hard Scattering: (Perturbatively Calculable)

Experimental Input

Parton Distributions:
Nonperturbative parametrization at Q_0
DGLAP Evolution to Q

The QCD global fitting procedure

1. Parametrize the PDFs $f_a(x, \mu_0)$ at a small μ_0 by smooth functions with lots of free parameters $\{A_i\}$.

2. Calculate $f_a(x, \mu)$ at all $\mu > \mu_0$ by DGLAP.

3. Calculate $\chi^2 = \sum_i [(\text{data}_i - \text{theory}_i)/\text{error}_i]^2$ to measure of the quality of fit to a large variety of experiments.

4. Obtain the best estimate of the true PDFs by varying the free parameters to minimize χ^2.

5. The PDF Uncertainty Range is assumed to be the region in $\{A_i\}$ space where χ^2 is sufficiently close to the minimum: $\chi^2 < \chi^2_{\text{min}} + \Delta\chi^2$.

Kinematic region of ep and μp data

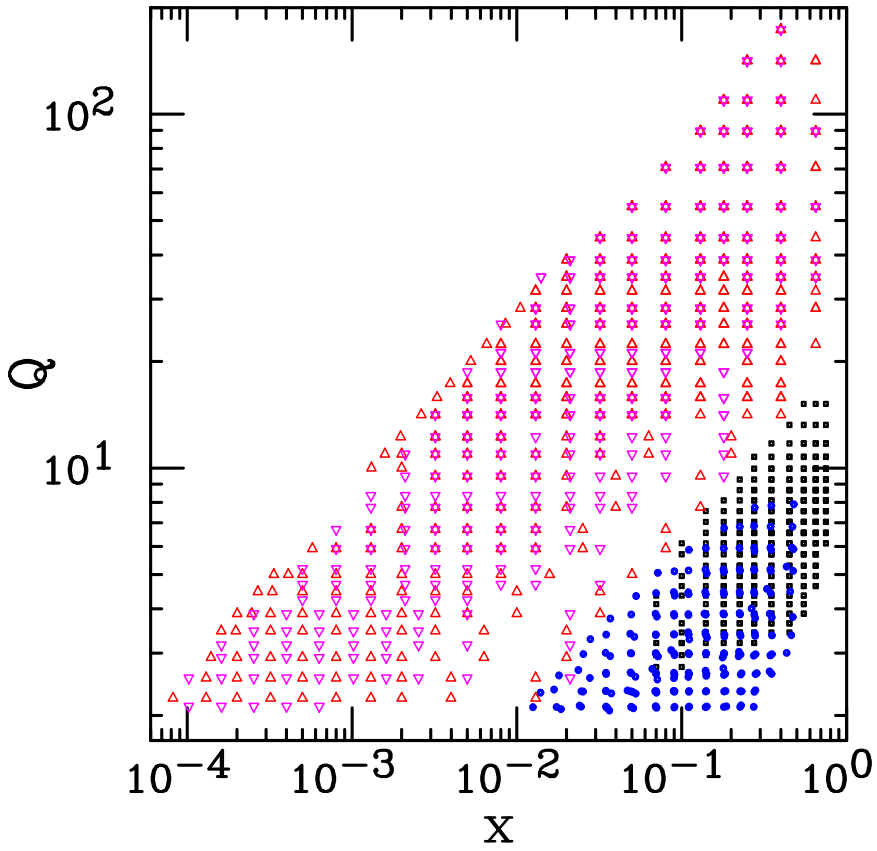

$ep \to eX$ (H1 = Δ, ZEUS = ∇)

$\mu p \to \mu X$ (BCDMS= box, NMC = $\circ$)

Drell-Yan data, neutrino DIS, and Tevatron W and Z data are also very important for differentiating among different flavors.

Tevatron inclusive jet data are very important for constraining the gluon distribution.

PDF results at 2 GeV and 100 GeV

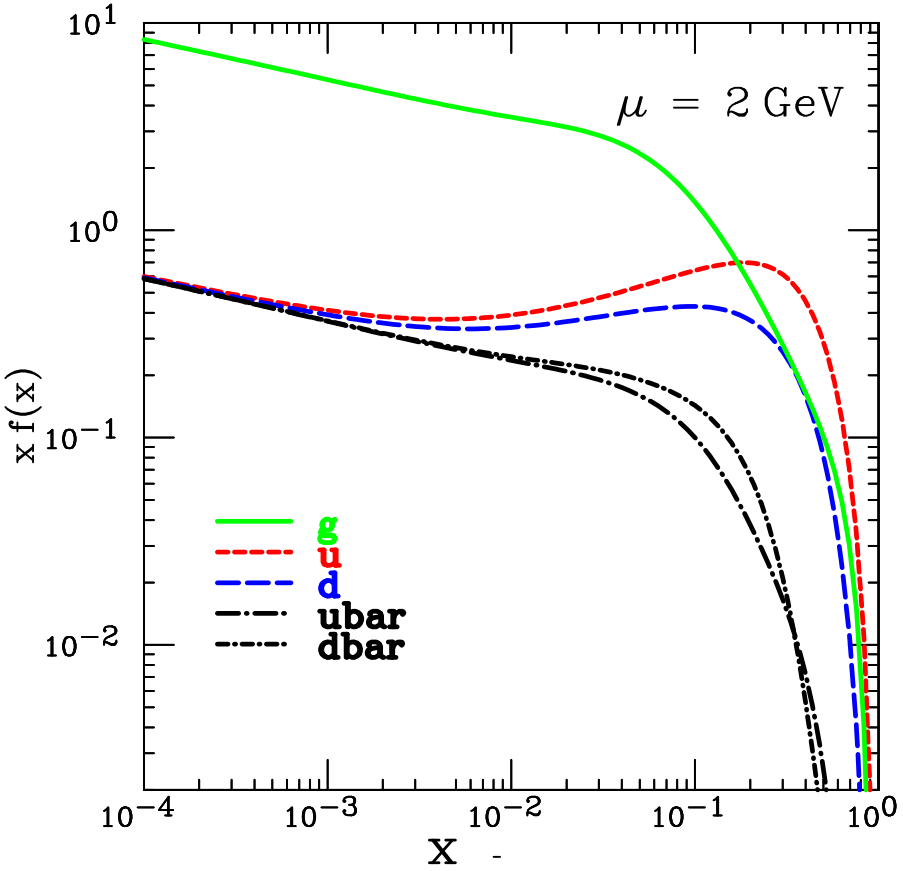

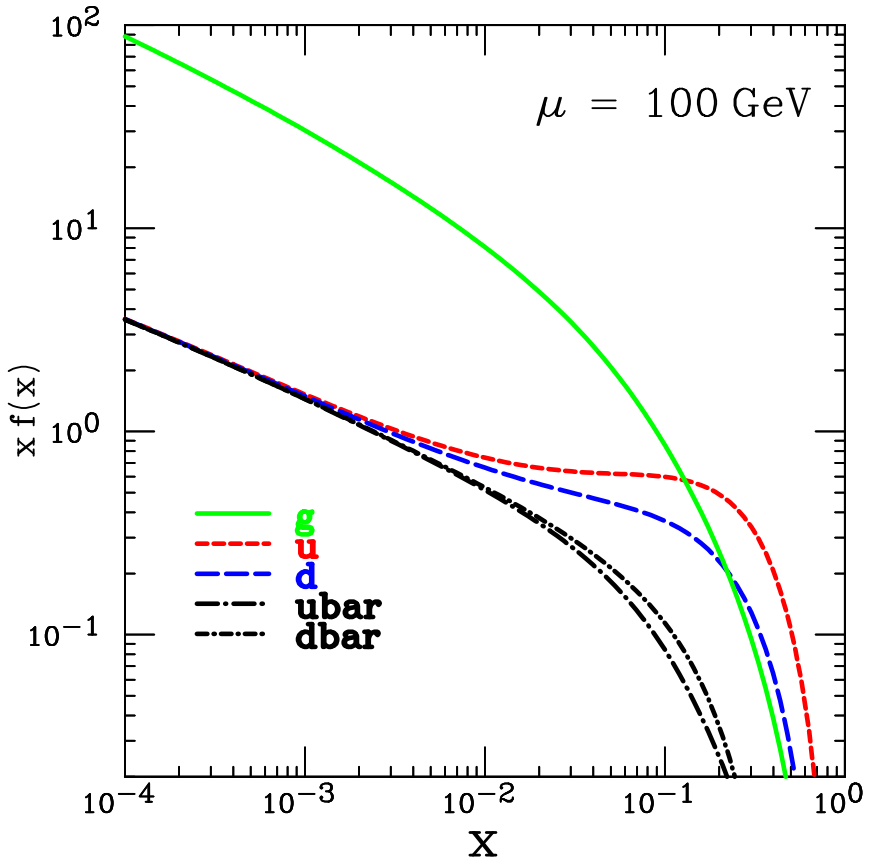

- Valence quarks dominate for $x \to 1$
- $u > d$ because $N_u = 2$, $N_d = 1$.
- Gluon dominates for $x \to 0$, especially at large μ.
- $\bar{u}$ and $\bar{d}$ are different — they even cross over.
- $u = \bar{u} = d = \bar{d}$ at $x \to 0$ is imposed in the parametrization, but is consistent with the data: dropping it allows very little reduction in χ^2.

DGLAP and Small x

Regge behavior of $\bar{u}$

The Regge behavior $x\,\bar{u}(x,\mu) \propto x^{a_1}$ that we assume for $x \to 0$ at μ_0 is quite well preserved by DGLAP evolution. This can be seen by the nearly straight-line behavior on a log-log plot, with slope nearly independent of μ:

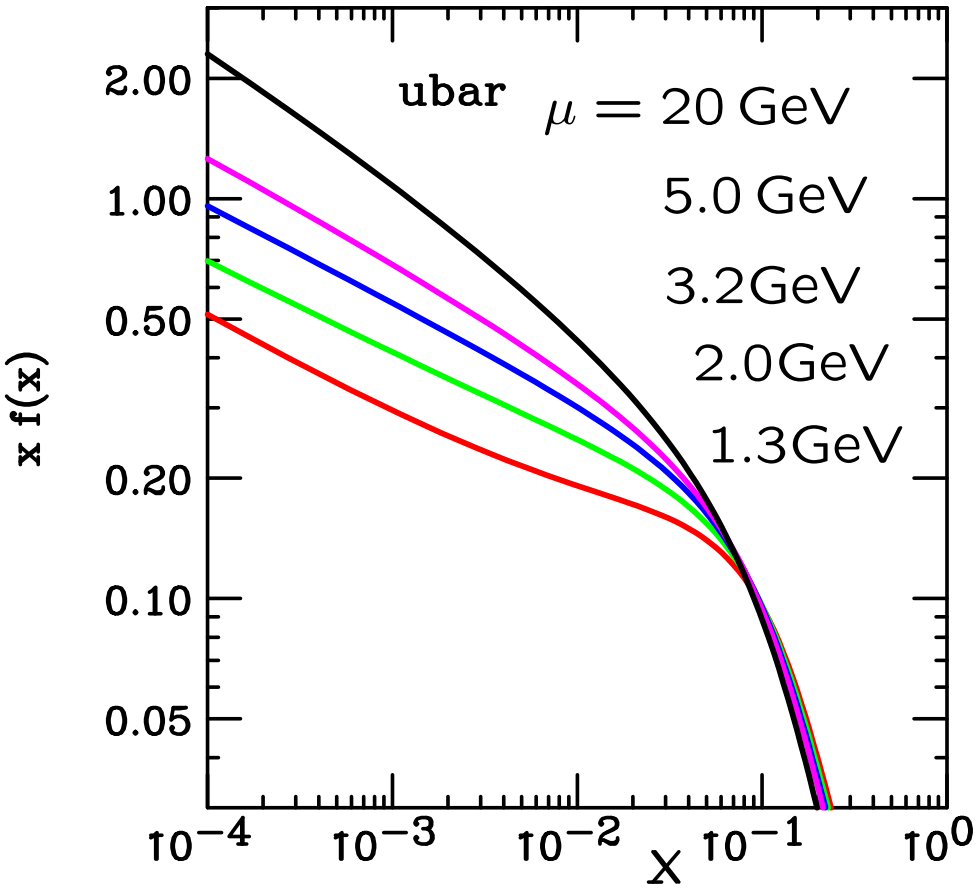

Numerical value of the slope a_1 agrees well with expectations from Regge, which supports the use of the $x\,\bar{u}(x,\mu) \propto x^{a_1}$ ansatz.

Regge behavior of $u_v \equiv u - \bar{u}$

The Regge behavior $x\,u_v(x,\mu) \propto x^{a_1}$ that we assume for $x \to 0$ at μ_0 is also well preserved by DGLAP evolution:

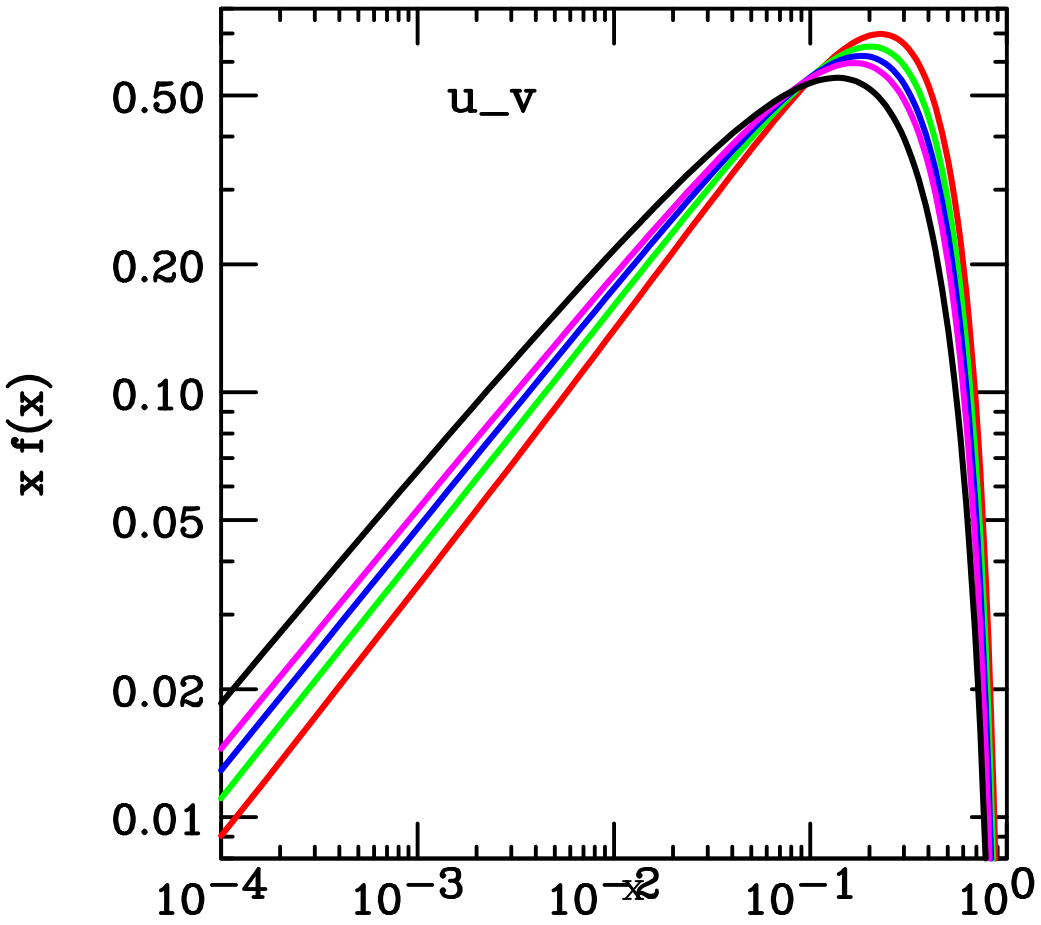

Again the observed slope value a_1 is consistent with expectations from Regge theory, which supports the choice of functional form.

Regge behavior of gluon at small x?

In contrast to valence and sea quark distributions, the NLO evolution of the gluon distribution at small x is very rapid. Hence no simple comparison can be made with expectations from Regge theory:

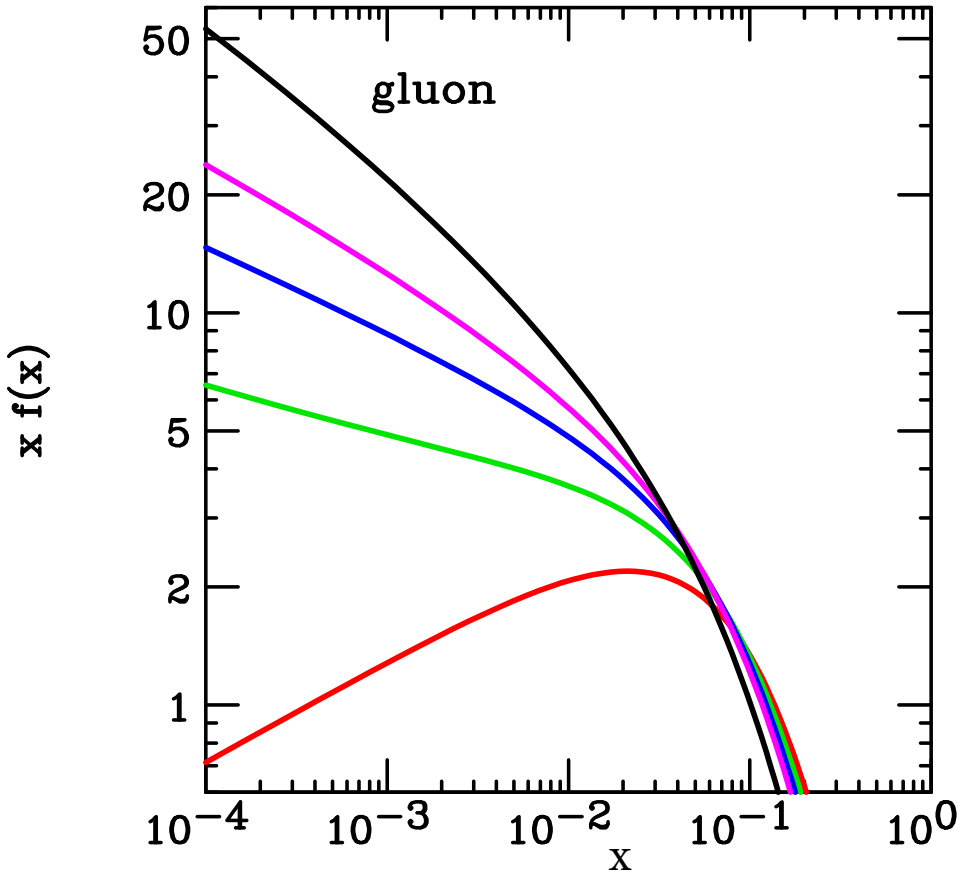

Perhaps this behavior is dictated by the rapid rise of F_2 seen at small x at HERA.

Or perhaps it shows that resummation corrections to DGLAP are needed as small x.

Excerpts from a talk on Uncertainties of PDFs

Measuring internal consistency of the fit

Partition the data into two subsets:

$$\chi^2 = \chi^2_S + \chi^2_{\overline{S}}$$

where subset S can, for example, be chosen as

- any single experiment
- all of the jet experiments
- all of the low-Q data points (to look for higher twist)
- all of the low-x data points (to look for BFKL)
- all experiments with deuteron corrections
- all of the neutrino experiments (to look for nuclear corrections)

A method I call Data Set Diagonalization which was first proposed in my HERA/LHC talk (March 2004) directly answers the questions

1. What does subset S measure?
2. Is subset S consistent with the rest of the data?

Data Set Diagonalization

The DSD method is an extension of the Hessian method. It works by transforming the contributions χ^2_S and $\chi^2_{\overline{S}}$ to χ^2 into a form where they can be interpreted as independent measurements of N quantities.

The essential point is that the linear transformation that leads to

$$\chi^2 = \chi^2_0 + \sum_{i=1}^{N} z_i^2$$

is not unique, because any further orthogonal transform of the z_i will preserve it. Such an orthogonal transformation can be defined using the eigenvectors of any symmetric matrix. After this second linear transformation of the coordinates, the chosen symmetric matrix will then be diagonal in the resulting new coordinates.

This freedom is exploited in the DSD method by taking the symmetric matrix from the quadratic form that describes the contribution to χ^2 from the subset S of the data that is chosen for study. Then . . .

DSD method – continued

$$\chi^2 = \chi^2_S + \chi^2_{\overline{S}} + \text{const}$$

$$\chi^2_S = \sum_{i=1}^{N} [(z_i - A_i)/B_i]^2$$

$$\chi^2_{\overline{S}} = \sum_{i=1}^{N} [(z_i - C_i)/D_i]^2$$

This decomposition answers the question "What is measured by data subset S?" — it is those parameters z_i for which the $B_i \lesssim D_i$. The fraction of the measurement of z_i contributed by S is

$$\gamma_i = \frac{D_i^2}{B_i^2 + D_i^2}.$$

The decomposition also measures the compatibility between S and the rest of the data $\overline{S}$: the disagreement between the two is

$$\sigma_i = \frac{|A_i - C_i|}{\sqrt{(B_i^2 + C_i^2)}}.$$

Experiments that provide at least one measurement with $\gamma_i > 0.1$

Process	Expt	N	$\sum_i \gamma_i$
$e^+ p \to e^+ X$	H1 NC	115	2.10
$e^- p \to e^- X$	H1 NC	126	0.30
$e^+ p \to e^+ X$	H1 NC	147	0.37
$e^+ p \to e^+ X$	H1 CC	25	0.24
$e^- p \to \nu X$	H1 CC	28	0.13
$e^+ p \to e^+ X$	ZEUS NC	227	1.69
$e^+ p \to e^+ X$	ZEUS NC	90	0.36
$e^+ p \to \nu X$	ZEUS CC	29	0.55
$e^+ p \to \bar{\nu} X$	ZEUS CC	30	0.32
$e^- p \to \nu X$	ZEUS CC	26	0.12
$\mu p \to \mu X$	BCDMS F_2p	339	2.21
$\mu d \to \mu X$	BCDMS F_2d	251	0.90
$\mu p \to \mu X$	NMC F_2p	201	0.49
$\mu p/d \to \mu X$	NMC F_2p/d	123	2.17
$p\,\mathrm{Cu} \to \mu^+\mu^- X$	E605	119	1.52
$pp, pd \to \mu^+\mu^- X$	E866 pp/pd	15	1.92
$pp \to \mu^+\mu^- X$	E866 pp	184	1.52
$\bar{p}p \to (W \to \ell\nu)X$	CDF I Wasy	11	0.91
$\bar{p}p \to (W \to \ell\nu)X$	CDF II Wasy	11	0.16
$\bar{p}p \to \mathrm{jet}\, X$	CDF II Jet	72	0.92
$\bar{p}p \to \mathrm{jet}\, X$	D0 II Jet	110	0.68
$\nu Fe \to \mu X$	NuTeV F_2	69	0.84
$\nu Fe \to \mu X$	NuTeV F_3	86	0.61
$\nu Fe \to \mu X$	CDHSW	96	0.13
$\nu Fe \to \mu X$	CDHSW	85	0.11
$\nu\,\mathrm{Fe} \to \mu^+\mu^-\mathrm{X}$	NuTeV	38	0.68
$\bar{\nu}\,\mathrm{Fe} \to \mu^+\mu^-\mathrm{X}$	NuTeV	33	0.56
$\nu\,\mathrm{Fe} \to \mu^+\mu^-\mathrm{X}$	CCFR	40	0.41
$\bar{\nu}\,\mathrm{Fe} \to \mu^+\mu^-\mathrm{X}$	CCFR	38	0.14

Total of $\sum \gamma_i = 23$ is close to actual number of fit parameters.

H1+ZEUS measure 6.2 of the parameters — fewer than in HERA-only fits as expected.

Consistency tests: measurements that conflict strongly with the other experiments ($\sigma_i > 3$) are shown in red.

Expt	$\sum_i \gamma_i$	(γ_1, σ_1), (γ_2, σ_2), ...
H1 NC	2.10	(0.72, 0.01) (0.59, 3.02) (0.43, 0.20) (0.36, 1.37)
H1 NC	0.30	(0.30, 0.02)
H1 NC	0.37	(0.21, 0.06) (0.16, 0.83)
H1 CC	0.24	(0.24, 0.00)
H1 CC	0.13	(0.13, 0.00)
ZEUS NC	1.69	(0.45, 3.13) (0.42, 0.32) (0.35, 3.20) (0.29, 0.80) (0.18, 0.64)
ZEUS NC	0.36	(0.22, 0.01) (0.14, 1.61)
ZEUS CC	0.55	(0.55, 0.04)
ZEUS CC	0.32	(0.32, 0.10)
ZEUS CC	0.12	(0.12, 0.02)
BCDMS F_2p	2.21	(0.68, 0.50) (0.63, 1.63) (0.43, 0.80) (0.34, 4.93) (0.13, 0.94)
BCDMS F_2d	0.90	(0.32, 0.67) (0.24, 2.49) (0.19, 2.09) (0.16, 5.22)
NMC F_2p	0.49	(0.20, 4.56) (0.17, 4.76) (0.12, 0.50)
NMC F_2p/d	2.17	(0.61, 1.11) (0.56, 3.60) (0.43, 0.90) (0.36, 0.79) (0.21, 1.41)
E605 DY	1.52	(0.91, 1.29) (0.38, 1.12) (0.23, 0.31)
E866 pp/pd	1.92	(0.88, 0.57) (0.69, 1.15) (0.35, 1.80)
E866 pp	1.52	(0.75, 0.04) (0.39, 1.79) (0.23, 1.94) (0.14, 3.57)
CDF Wasy	0.91	(0.57, 0.33) (0.34, 0.51)
CDF Wasy	0.16	(0.16, 2.84)
CDF Jet	0.92	(0.48, 0.47) (0.44, 3.86)
D0 Jet	0.68	(0.39, 1.70) (0.29, 0.76)
NuTeV F_2	0.84	(0.37, 2.75) (0.29, 0.42) (0.18, 0.97)
NuTeV F_3	0.61	(0.30, 0.50) (0.16, 1.35) (0.15, 0.30)
CDHSW	0.13	(0.13, 0.04)
CDHSW	0.11	(0.11, 1.32)
NuTeV	0.68	(0.39, 0.31) (0.29, 0.66)
NuTeV	0.56	(0.32, 0.18) (0.24, 2.56)
CCFR	0.41	(0.24, 1.37) (0.17, 0.12)
CCFR	0.14	(0.14, 0.79)

Measurements in a recent PDF fit

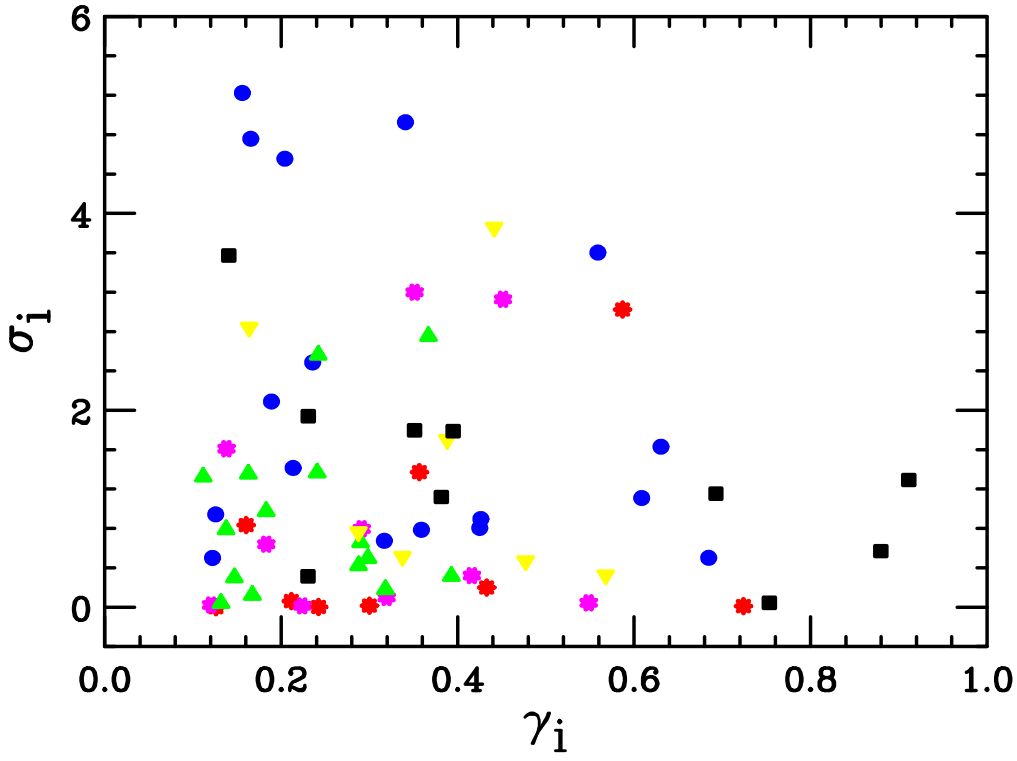

Figure showing the results in the table.

ep (daisy);

$\mu p, \mu d$ (○);

pp, pd, pCu (box);

$\bar{p}p$ (∇);

νA (Δ).

Consistency of measurements in a global fit

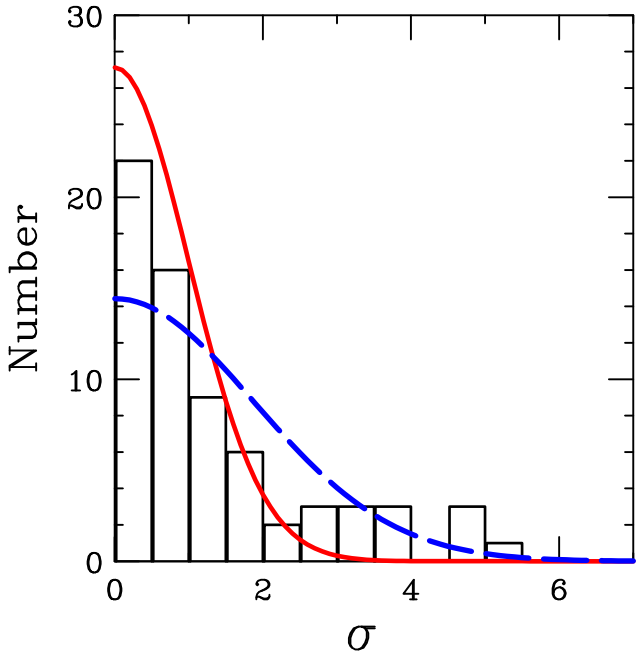

Histogram of the consistency measure σ_i for the 68 significant ($\gamma_i > 0.1$) measurements provided by the 37 experiments in a typical global fit.

Solid curve is the absolute Gaussian prediction

$$\frac{dP}{d\sigma} = \sqrt{\frac{2}{\pi}}\,\exp(-\sigma^2/2)\,.$$

Dashed curve is a scaled Gaussian with $c = 1.9$:

$$\frac{dP}{d\sigma} = \sqrt{\frac{2}{\pi\, c^2}}\,\exp(-\sigma^2/(2\,c^2))$$

Conclude: Disagreements among the experiments are larger than predicted by standard Gaussian statistics; but less than a factor of 2 larger.

Conclusion from the consistency study

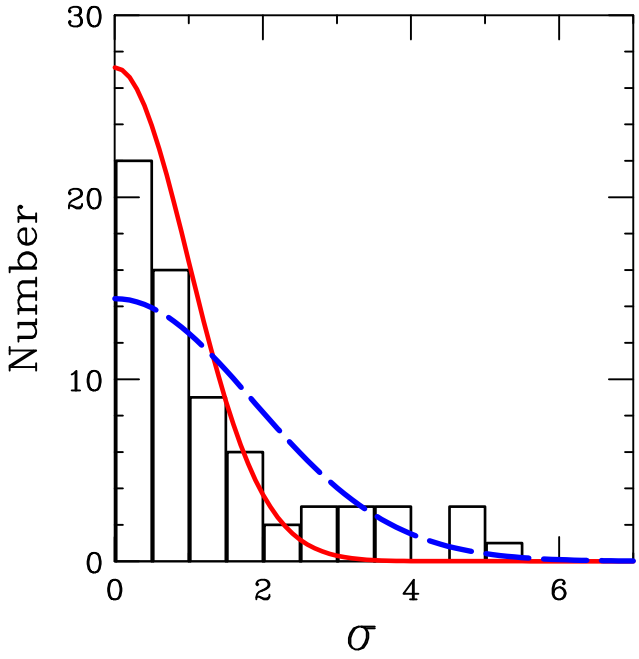

This fit provided direct evidence of a significant source of discrepancy associated with fixed-target DIS experiments for large x at small Q. (Higher-twist effects had been seen there previously; but not taken into account in PDF fitting — at least by CTEQ.) Removing those data by a kinematic cut makes the average disagreement smaller, but it still does not become consistent with the absolute Gaussian.

In hep-ph/0909.0268, I argue that this suggests a "tolerance criterion" $\Delta\chi^2 \approx 10$ for 90% confidence uncertainty estimation. It is possible that other uncertainties in the analysis require larger $\Delta\chi^2$; but the experimental inconsistencies do not.

Studies relating to the choice of $\Delta\chi^2$

It is important to know if we are underestimating or overestimating the PDF uncertainties.

For properties that we have little information, the Hessian method generally underestimates uncertainties, because completely unknown behavior requires parametrizations assumptions for convergence. However, fortunately, this is generally not too important because the properties that present-day PDF data are insensitive to are also generally unimportant for LHC phenomenology. Example: $u(x) - \bar{u}(x)$ at small x is poorly known, and also unimportant.

Will discuss this further in the PDF4LHC workshop.

Sum rule tests

A direct test of the treatment of uncertainties can be made by treating the valence quark numbers and/or the total partonic momentum as free parameters in the fit, since for these cases we know the true answer exactly:

$$N_u = \int_0^1 [u(x) - \bar{u}(x)]\, dx \qquad \text{SM value} = 2$$

$$N_d = \int_0^1 [d(x) - \bar{d}(x)]\, dx \qquad \text{SM value} = 1$$

$$m = \sum_a \int_0^1 f_a(x)\, x\, dx \qquad \text{SM value} = 1$$

(These are scale-independent under DGLAP.)

If m only is set free, it moves to 1.025 with a reduction of 5 in χ^2.

If N_u and N_d are set free, they run to 2.6 and 1.3 with a reduction of 10 in χ^2.
(N_u and N_d are not well determined in the global fit, because the data are insensitive to $u(x) - \bar{u}(x)$ and $d(x) - \bar{d}(x)$ at small x, where these quantities are much smaller than $\bar{u}(x)$ and $\bar{d}(x)$.)

Sum rule tests – continued

If all three are set free, the fit prefers

$$N_u = 2.8 \qquad N_d = 1.5 \qquad m = 1.03$$

with χ^2 lower by 15.

Hence we do not want to think of $\Delta\chi^2 = 15$ as a significant improvement — at least for the prediction of quantities that are poorly determined.

Uncertainty example: Light Gluino

(E. Berger, P. Nadolsky, F. Olness and J. P., Phys. Rev. D **71**, 014007 (2005)

Hypothesizing a gluino of mass $\sim 10\,\mathrm{GeV}$ improved a previous global fit by ~ 25 units in χ^2.

We took this an intriguing possible hint for plausible New Physics. But you would be crazy to consult a statistical table of χ^2 probabilities and declare it inescapable.

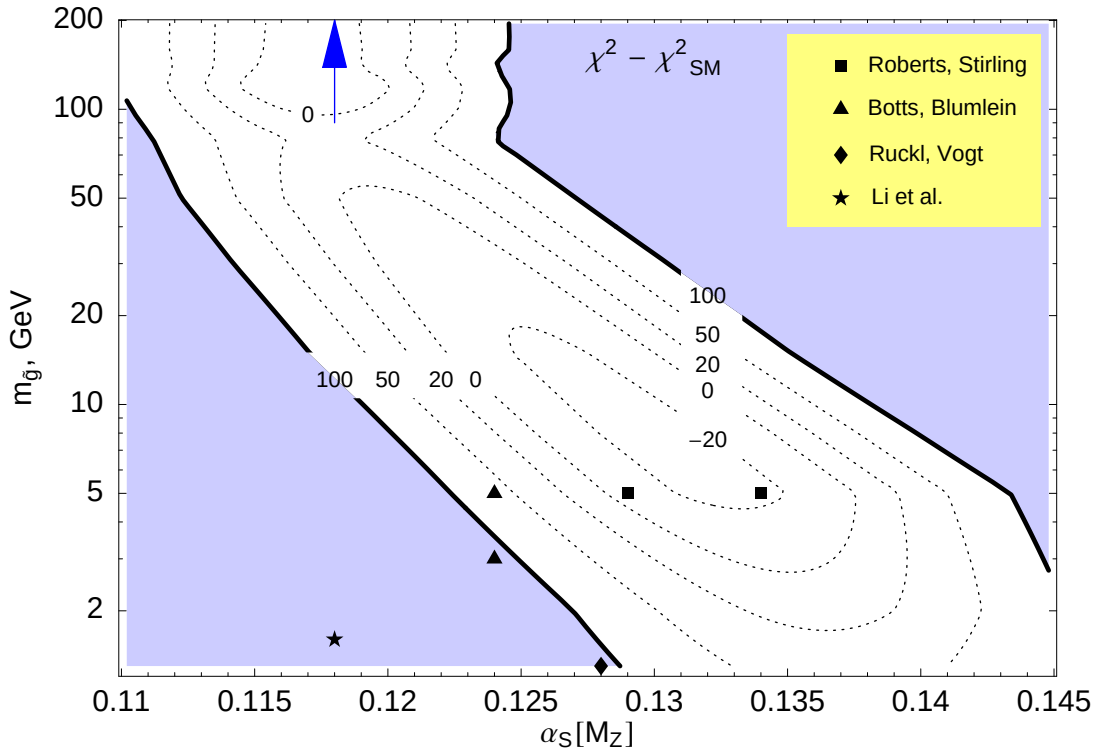

Parametrization dependence at large x

Our standard fitting procedure adds a penalty to χ^2 to force "expected" behavior for the gluon distribution at large x: $1.5 < a_2 < 10$ in

$$x\,g(x,\mu_0) = a_0\,x^{a_1}\,(1-x)^{a_2}\,\exp(a_3\sqrt{x} + a_4 x + a_5 x^2)$$

Figure shows the $\Delta\chi^2 = 10$ uncertainty range.

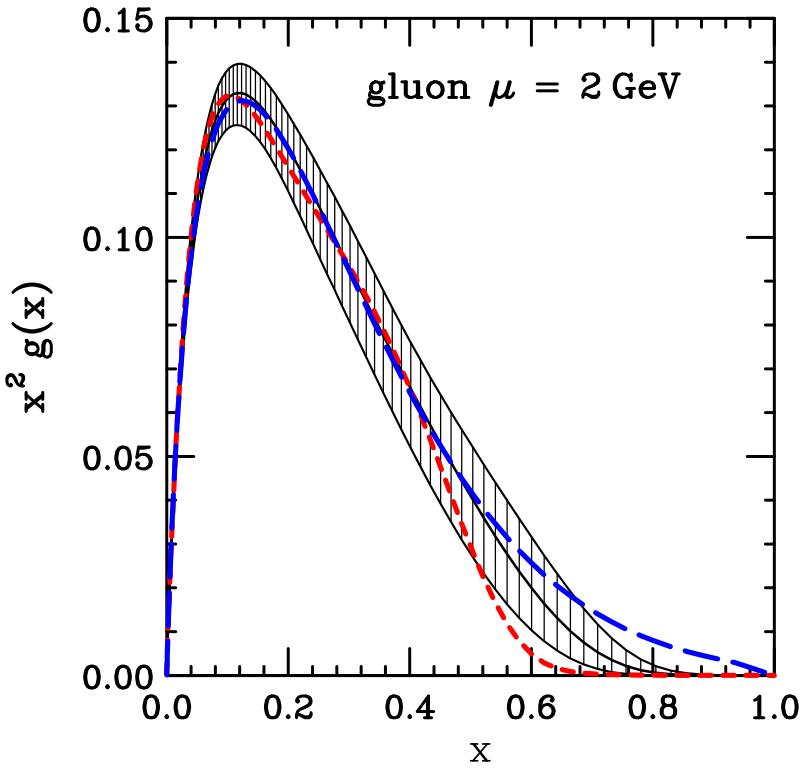

Curves show $a_2 = 54$ (which produces $\Delta\chi^2 = 10$) and $a_2 = 0$ (which requires almost zero $\Delta\chi^2$)

Non-perturbative theory constraints are important at large x.

Parametrization dependence at small x

Figure shows $\Delta\chi^2 = 10$ uncertainties. Curves show results of alternative parametrizations that enhance or suppress the gluon at small x

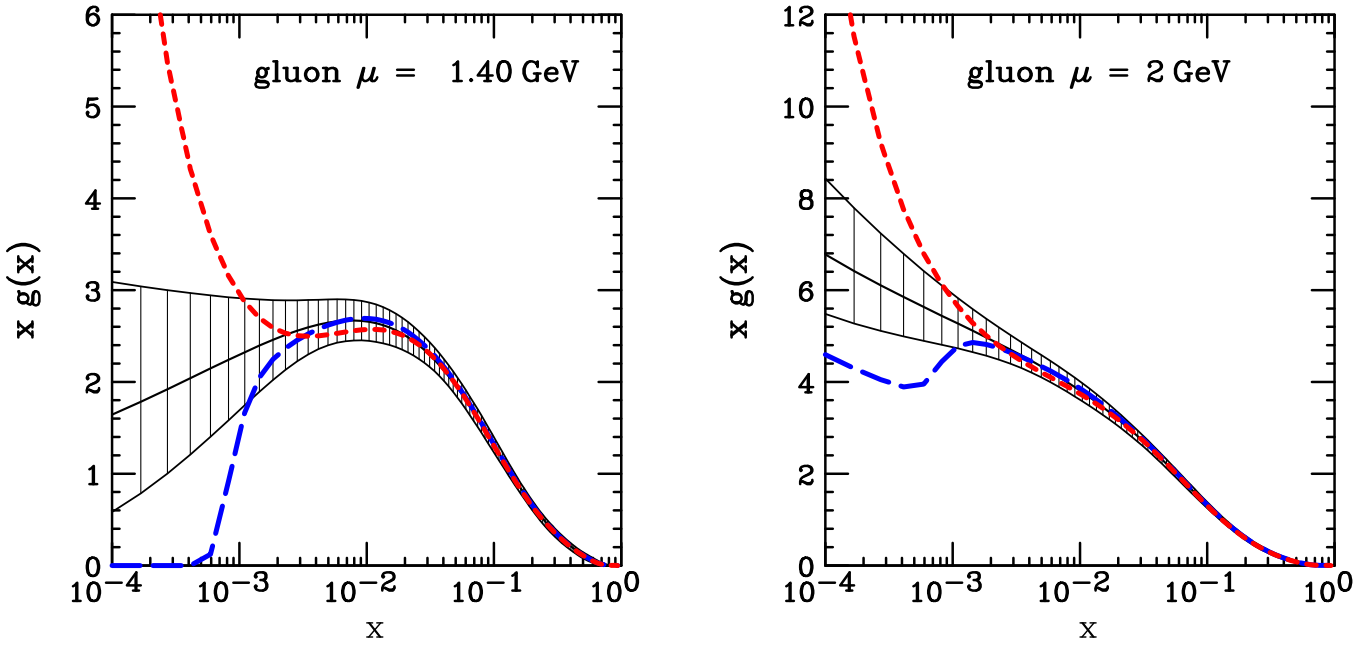

In a region where the data provide little constraint, the true uncertainty is much larger than $\Delta\chi^2$ shows because of parametrization dependence.

There is very little constraint on gluon at small x for low scale μ; but at higher scales, the small-x gluon is generated mainly by DGLAP evolution down from higher x, so the uncertainties – e.g. for heavy objects created from gluons at LHC – are not so large.

Parametrization dep. at intermediate x

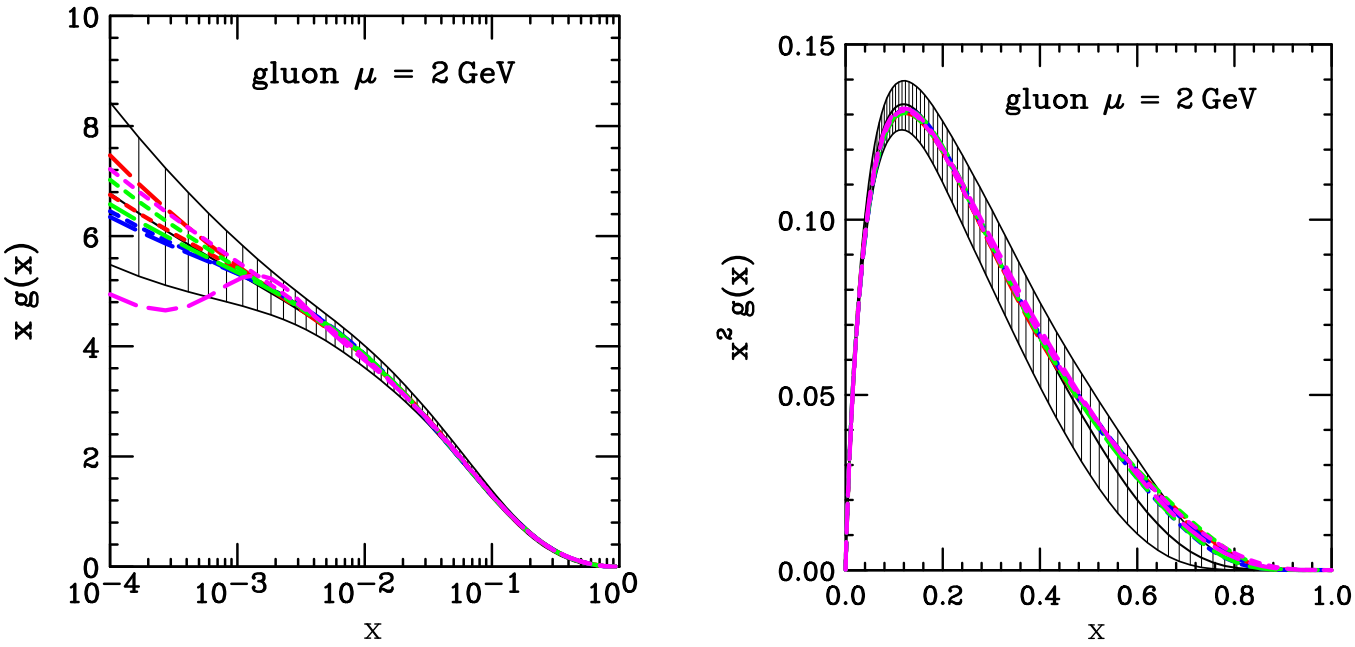

Figures show gluon uncertainty at $\Delta\chi^2 = 10$.

Curves show results from alternative parametrizations with up to 8 more parameters added.

The added freedom reduces χ^2 by as much as 10 – 15, but the change in the gluon distribution is small except at extreme x — where we already knew there was substantial parametrization dependence.

"Time dependence" of PDFs

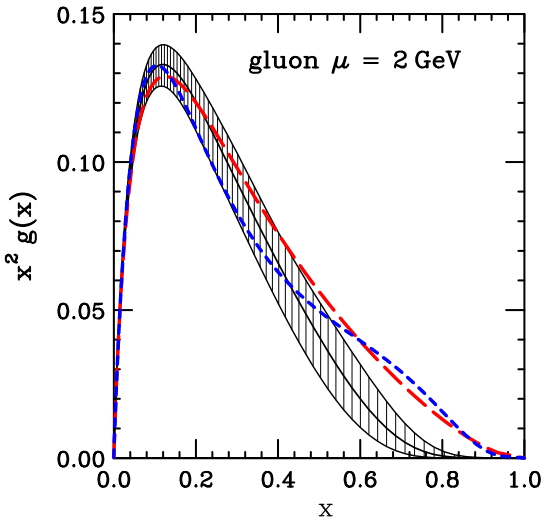

$\Delta\chi^2 = 10$ uncertainties in a recent fit (all weights 1.0; run II jet data only).

CTEQ6.6 central fit: used run I jet data only; different weights for different experiments.

CT09 central fit: used both run I and run II jet data; different weights for different experiments.

It is clear that $\Delta\chi^2 = 1$ for 68% confidence would be overly optimistic.

It appears that $\Delta\chi^2 = 10$ may be (nearly?) large enough, in regions where the data provide substantial constraint.

(Larger time-dependence would be seen for earlier PDFs because of improving treatments, e.g. of heavy quarks after CTEQ6.1.)

"Space dependence" of PDFs

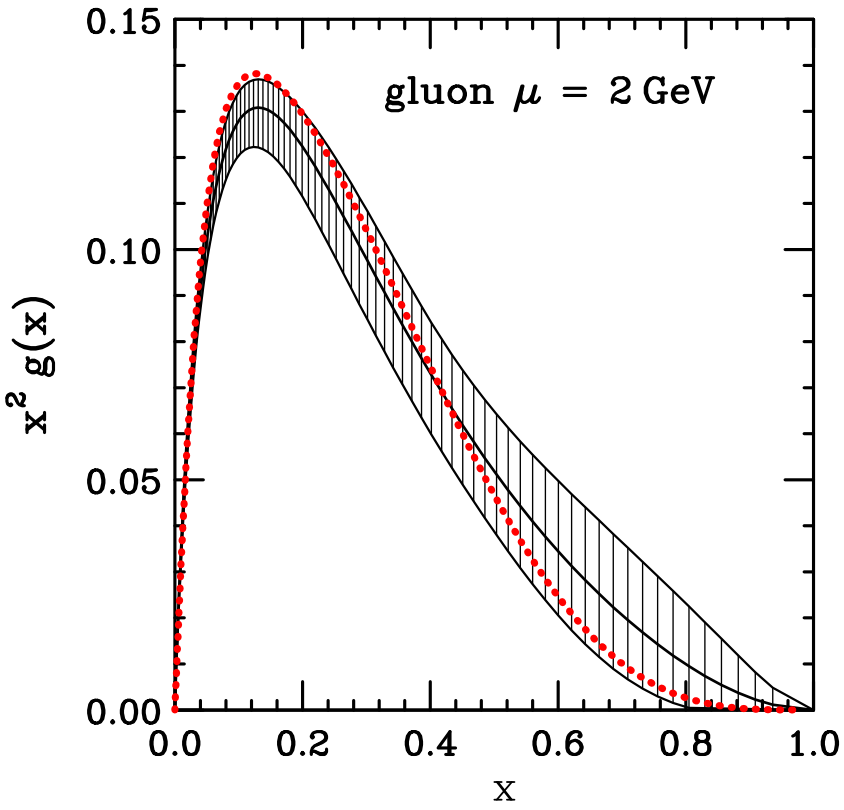

$\Delta\chi^2 = 10$ uncertainties in a recent fit (All weights 1.0; no run I jet data, $\alpha_s(m_Z) = 0.12018$ to match MSTW.)

MSTW2008 central fit

Again it is clear that $\Delta\chi^2 = 1$ for 68% confidence would be overly optimistic.

Again it appears that $\Delta\chi^2 = 10$ may be (nearly?) big enough in regions where the data provide substantial constraint.

Conclusion

- There is an active ongoing program to determine the PDFs that are needed for LHC.
- As befits a critical mission component, there are several groups working independently on the problem.
- Estimating the size of the uncertainties caused by systematic errors in the theory is a current hot topic in which further progress can be expected.

To illustrate how easy it is to access the PDFs, a final figure was obtained by a few clicks on
`http://durpdg.dur.ac.uk/hepdata/pdf3.html`

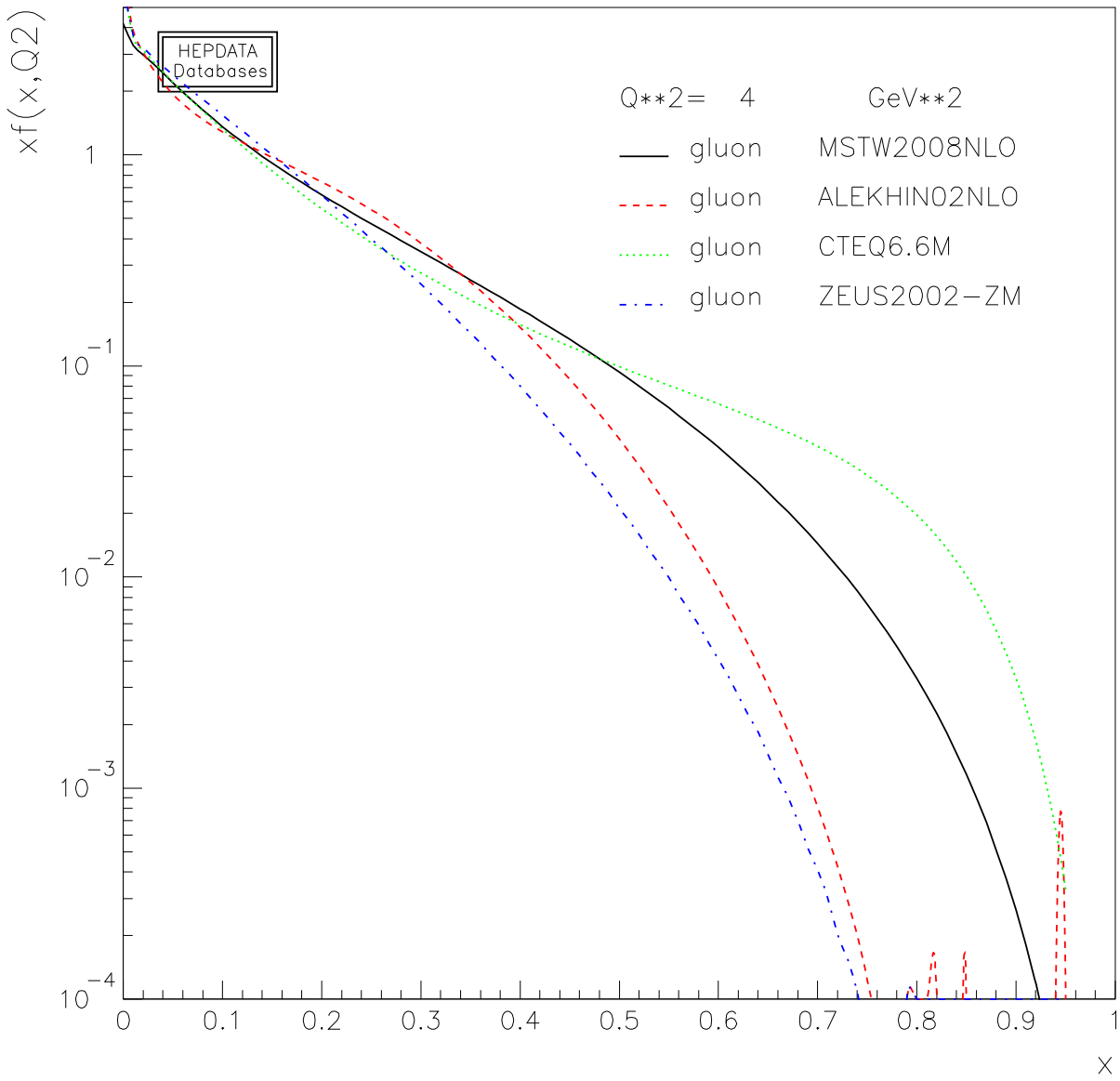
HEPDATA
Databases
Q**2= 4 GeV**2
gluon MSTW2008NLO
gluon ALEKHIN02NLO
gluon CTEQ6.6M
gluon ZEUS2002−ZM
xf(x,Q2)
1
10^−1
10^−2
10^−3
10^−4
0
0.1
0.2
0.3
0.4
0.5
0.6
0.7
0.8
0.9
1
X